Development of the Floorball

Product development focused on sport ball for floorball, with the aim to suggest new designs mainly concerning the improvement of a high-performance ball for indoor play.

by

SARA MATEOS FERNÁNDEZ

Diploma work No. 169/2015
Department of Materials and Manufacturing Technology
CHALMERS UNIVERSITY OF TECHNOLOGY
Gothenburg, Sweden

Diploma work in the Master program Mechanical Engineering

Performed at: Department of Materials and Manufacturing Technology
Chalmers University of Technology
SE-41296 Gothenburg, Sweden

Examiner: Professor Antal Boldizar
Department of Materials and Manufacturing Technology
Chalmers University of Technology, SE - 412 96 Gothenburg

Development of the Floorball

Product development focused on sport ball for floorball, with the aim to suggest new designs mainly concerning the improvement of a high-performance ball for indoor play.

SARA MATEOS FERNÁNDEZ

Development of the Floorball

Product development focused on sport ball for foorball, with the aim to suggest new designs mainly concerning the improvement of a high-performance ball for indoor play.

SARA MATEOS FERNÁNDEZ
Department of Materials and Manufacturing Technology
Chalmers University of Technology

SUMMARY

As a relatively new sport, the research specifically aimed at developing the game of floorball is limited. The aim of this thesis work was to develop a high performance ball while achieving as much as possible the requirements of International Floorball Federation (IFF). Based on a CAD model of the current design of the ball, some interesting variations of the geometry were introduced as a first approach. The alternative geometries studied were variations of surface dimples and hole geometries. Simulations were reproduced with CFD in order to study the aerodynamic parameters involved in the predictability of the flight. The most promising ball geometry was selected for prototypes made of polyamide and produced with an additive manufacturing technique. The flight performance of the prototypes was then studied by analysing the recorded ball trajectories. In an effort to further evaluate the performance of the prototype, compared with the other precision balls, parameters such as speed and aerodynamic coefficients were experimentally calculated. The major finding in this work was that the modified geometry of the holes of the ball may lead to a more predictable shot. The results suggest new improved ball designs having smaller hole diameter and hole edges with an inside chamfer.

Contents

Index of Figures

List of Acronyms

IFF	International Floorball Federation Three Dimension (s/al)
SP	Technical Research Institute of Sweden
3D	Three Dimension (s/al)
CAD	Computer Aided Manufacturing
CFD	Computational Fluid Dynamics
AM	Additive Manufacturing

1. Introduction

The main motivation of this project was the intention of the International Floorball Federation to explore the possibilities for further development for both improved indoor play as well as outdoor play. This topic constitutes a significant challenge in terms of both Materials and Manufacturing Technology, involving both traditional and modern manufacturing technologies as well as exploring possibilities with new product design. In the following sections, information from certification organisms, manufacturers and experts in manufacturing technologies are collected in order to obtain a reasonable background for this work.

1.1. Aim of the work

The aim of this thesis work was to develop a high performance ball, with different designs for both inside and outside playing, while achieving as much as possible the requirements of International Floorball Federation (IFF). The high-performance ball designed indoor games should aim for improved predictability during rolling and improved joining of the ball halves for better mechanical durability and balance. The development of a ball for outdoor games should be designed with special attention to the wear problem on asphalt and the sensitivity to windy conditions.

1.2. Background

Originally, floorball started as a game played for fun and at schools, but in late 1980´s it became a developed sport with formal rules and national associations mostly in Nordic countries. In 1986, the International Floorball Federation (IFF) was formed by joining the associations of Finland, Sweden and Switzerland.

A major responsibility of IFF is the development of equipment to be used at regulated games. For this reason, IFF has published the specific criteria in the *Material Regulations* where all the requirements for certification and marking are collected. The certification system is managed by the Technical Research Institute of Sweden (SP) to operate according to adopted rules for testing and approval of floorball equipment (1).

Since the creation of IFF, this sport has increased substantially in many other regions of the world, according to annual statistics (2), rising above 300.000 licensed players at the end of 2014. The development of this sport is attracting interest from developing countries as it does not need much material or infrastructure for playing. However, the present equipment in regulation can likely be better adapted to improved performance for outdoor conditions.

To similar backgrounds a group at Chalmers has been formed for promoting Sports Technology in general (3). From 2012, several seminars and research projects in collaboration with professionals of different sports have been started. Seminars have been held, concerning Floorball, known in Sweden as Innebandy, on the topic of spreading the sport to developing countries and how to improve the conditions for outdoor games. Such a development would involve more investments in the development of the better adapted equipment, here naturally making use of recent advances in materials technology and engineering solutions.

1.3. State of Art

There has been a substantial development of floorball equipment, most of it regarding competition equipment, which requires precision balls and high performance products. With the purpose of learning from previous designers, experienced in this subject, a review of the existing floorball equipment has been carried out, finding an interesting point of departure for further development. Focusing the attention on basic equipment, only the stick and ball improvements have been studied concerning recent changes.

The sticks have been developed strongly, leading to light weight sticks and many different shapes for the blade according to the preferences of the player. Many materials have been used providing a range of stiffness and flexibility, with a current preference for composite materials for advanced players while more common polymers for beginners. There has been a great development of sticks and Chalmers University has collaborate to recreate a finite element model of a stick during a slap shot, leading to inputs for a better functionality of a new sticks generation , (4) (5).

The ball has a basic design with 26 holes with a fixed range of dimensions and weight, according to IFF requirements. Some modifications have been introduced during last years to improve the predictability of the ball trajectory. The basic balls have a smooth surface while the balls intended for competitions have more structured surfaces with dimples, similar to golf balls. This has been the most significant change in the development of floorball ball, resulting in a wide range of balls with dimpled surface on the market. The most revolutionary designs of precision balls came from two Swedish companies, settled near Göteborg.

The Aero+ ball from Salming, established in Askim, is claimed to have optimized dimples and stabilizer structure inside the ball, providing a more balance and predictable flight, Figure 1 (6). The present official ball for all IFF competitions (7) is design by Renew Group having a unique design with a surface structure having for the parallels and meridians, Figure 2 (8).

Figure 1. Aero+ Ball from Salming (6)   Figure 2. Crater Ball from Renew Group (8)

Through the study of previous designs, it is clear that the predictability of the ball movement depends on the aerodynamic parameters such as aerodynamic drag and turbulence of air inside ball, much depending on the type of holes. The reduction of aerodynamic drag also depends on surfaces, for instance by modifying the number and geometry of the dimples as a first approach to the better design. Some other designers have introduced additional features in their products in order to change the air flow inside the ball. For example the invention registered under the patent number WO/2012/126442 (9) divides the ball in different internal compartments trying to isolate the air flow to reduce turbulence.

1.4. Requirements for Approval

The products developed in this thesis work are proposed for precision balls; intended for official league matches. For this reason, the geometries need to adhere to the certification rules established by IFF.

The requirements are based on standards collected in the document *"Material Regulations Certification Rules for IFF-marking of Floorball Equipment SPCR 011"* (10) published by the official certification agency SP Technical Research Institute of Sweden. The procedures to follow during certification are explained in this publication as well as the requirements for the testing equipment. The requirements on the balls are mainly according to Table 1 and Figure 3.

Weight	23 ± 1 gr	**Surface Fineness**	Ra 1—5 μm
Diameter	72 ± 1 mm	**Number of Holes**	26
Diameter of holes	10 ± 1 mm	**Breaking stress**	6.0 N/mm^2
Hole's internal placement over joint	c/2 ± 2 mm	**Rebound**	650 ± 50 mm

Table 1. Ball Characteristics from SP Technical Research Institute of Sweden.
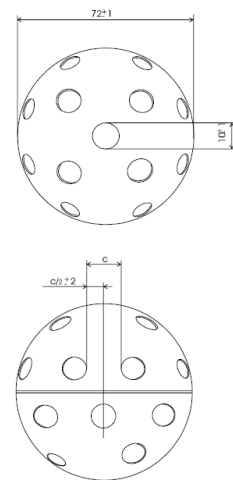
Figure 3. Dimension requirements for Floorball Ball from SP.

1.5. Manufacturing Process

The current manufacturing process of the Floorball balls consists of two steps:

– Shaping of half ball shells, generally by injection moulding
– Join of the shells, by welding

1.5.1. Injection moulding

This process has been used widely in industry for the manufacture of many different thermoplastic objects, such as containers, tool handles, toys, etc. It is a well-known process to manufacture a great amount of units with good accuracy results (11). The process consists of the injection of a plastic melt into a closed mould. The plastic will cool down, and replicate the mould surfaces, then will be ejected from the mould.

The machine consists of two units: injection unit and clamping unit. The injection unit generates the molten material and enough pressure for injection into the mould. The hopper feeds raw material into a combined barrel and a screw. The barrel is heated externally to help the melting of the plastic material, while also the pressure and friction inside the barrel generates a great amount of heat. The movement of the screw controls the material to be injected through the nozzle. The clamping unit consists of a holding mechanism to keep the mould closed during injection and eject the part when it has cooled down.

1.5.2. Plastic Welding

The joining of the shells is generally done by heated tool welding, also known as hot plate or mirror welding, which is a commonly used technique for joining injection moulded components.

This process consists of heating and melting the surfaces that are to be joined. Once the desired part is softened, the tool is removed and the components are pressed together with a specific force (12). This is a simple economical technique that makes hermetically welds both large and small parts. This welding requires a relatively long cycle time.

1.6. Additive Manufacturing

Regarding an improved joining of the shells, the idea was to study new manufacturing processes like Additive Manufacturing (AM), which allows the manufacture of a product in a single operation. Moreover, this technology has some advantages such as customization of products or the possibility of locally manufacture the balls.

It is common to call AM as Rapid Prototyping since this was the main purpose of this technology, settled in the early 80´s due to the development of similar technology based on CAM. The concept of Rapid Prototyping emphasizes the fast way to create a model representation before the manufacturing for commercialization, also reducing the costs of traditionally craft made prototypes. It is a good method to obtain prototype models directly from CAD data, which would be useful for this thesis work as the evaluation of alternative designs will be performed by testing the ball in game conditions.

Recent efforts to make of this technology a real possibility for final manufacturing have become the "fastest growing segment of the industry" (13) as the expert in the field Terry Wohlers announces in his annual report and some other publications. The same author declares that the industry is getting more confident on the results provided by these processes, therefore companies such as GE, Boeing or Airbus are developing projects based in this new technology for final products (14) .

The main advantage of AM is the possibility to build very complex geometries basically in one single step and without a previous and complicated process planning. It is not necessary to invest a large amount of time and resources to consider how the part can be manufactured, so making the geometry independent from the manufacturing process gives the possibility of customization and moreover the design for individual needs, such as the current trend for medical products (15).

1.7. Meeting the manufacturers

During the development of this research, I had the occasion to visit Elmia Polymer 2015, a trade fair focused on the industry of plastics in Jönköping (16). Most of the companies present at the exhibition were experts in processes such as injection moulding and extrusion, though there were a small number of companies that were developing their activity in the field of AM.

The exhibitors found at Elmia were specialized in Fused Deposition Modelling (FDM), Selective Laser Sintering (SLS) and Stereolithography (SLA) which are the most common AM processes. The staff from companies visited, ADDEMA (17) and Prototal (18), found it interesting to manufacture a floor ball with these technologies. The feedback was positive and they provided some advice regarding the choice of materials, which is not only based in the properties desired but also in the process used.

For instance, from the point of view of impact resistance, ABS is the best choice for FDM or SLA processes, meanwhile in the Selective Laser Sintering processes, when the aim is to achieve a great strength-weight ratio, there is the possibility to use some composites by mixing polyamide powder with carbon or glass fibres. Additionally to the more traditional AM processes, a new process was shown from the expert in injection moulding Arburg. The process, called Arburg Plastic Freeforming (19), consists of a melting system, similar to a rotating screw for injection moulding, which produces minuscule droplets to create products layer by layer. The great advantage of this new process is that standard plastics granulates can be used.

2. Design and Development

The general purpose of the project was to develop improvements for indoor and outdoor balls according to the schema in Figure 4.During the development of this work the efforts needed to be focused on a limited part of the scheme due to practical reasons.

Product Development					
Indoor Precision Ball				Outdoor Ball	
Predictability		Durability	Manufacturing	Outdoor Conditions	Wear Resistance
Aerodynamic Design	Dynamic SImulation	Maximize Stiffness	Alternative Process	Wind Influence	Material for Friction
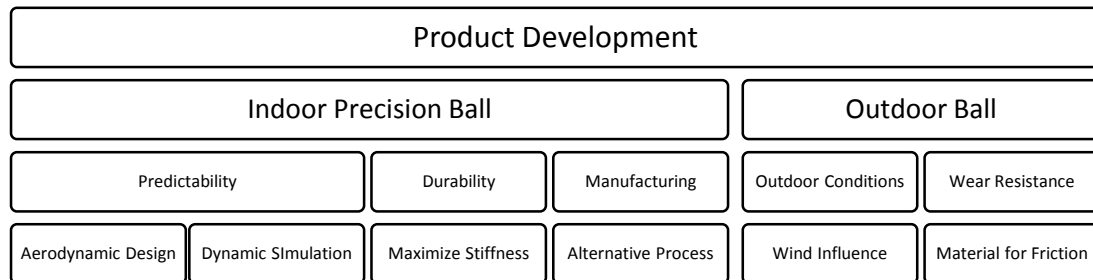
Figure 4. Areas of Work

Therefore, the results presented herein are mainly related to the improvement of the predictability of the ball for indoor games. The work done relates mainly to the aerodynamic behaviour of the ball through modifications of the geometry used on computer aided environment for fluid dynamics simulation.

2.1. Objectives

2.1.1. Improvement of Predictability

The previous improvements in this field show that there may be a possibility to achieve more predictable balls by improving the aerodynamic design and by studying the performance during the game.

After the revision of existing products, the manufacturers often mention the aerodynamic drag and air turbulence inside the ball as parameters to be reduced for a more predictable and stable flight. Therefore, further development was pursued by reconsideration of some basic aerodynamic concepts and how to apply them in the new design. In order to evaluate the results, it was interesting to perform a dynamic computer aided simulation of the ball behaviour.

2.1.2. Alternative Manufacturing Process

The improvement of the joining of the halves for a better mechanical durability can possibly be done by changing the current manufacturing process into a direct manufacturing of the ball without seams. It may be possible that the current manufacturing process does not allow making a more complex geometry of the final product. Additionally, if some internal features are added to the ball the selection of an Additive Manufacturing Process seems to be an interesting idea for a direct manufacturing.

2.1.3. Development of Outdoor ball

The need for an outdoor ball is related to the expansion of floorball to developing countries, where this sport is reaching high number of players. The initiatives from Floorball4all (20) encourage children and teenagers to play this sport as "prevention of addiction in the troubled neighbourhoods of this world" according to Hansjörg Kaufman, the man behind such a Project (21). Due to this high increase of outdoor players, it seems necessary that the development of an outdoor ball should include special features to achieve the highest performance in outdoor conditions, which are the wear caused by different ground surfaces and the influence of wind.

Since the outdoor ball is expected to be influenced by the environment considerably, the redesign was carried out regarding the sensitivity to wind as main drawback in the outdoor playing.

2.2. Aerodynamic Background

After the revision of literature about Floorball Equipment Development, it was clear that the interaction of the ball with the air requires a further analysis of the aerodynamic forces that affect the flight, and therefore the predictability of the ball. More specific literature about this question was studied to determine the main parameters involved in the flight of an object and more precisely in sports balls previously studied by Metha (22) and Goff (23).

The main aerodynamic theories involved in this study are presented in this section providing a better understanding of the concepts applied in the further design and analysis of the ball studied.

The aerodynamic forces have an important role in the flight of a ball through the air. The interest of knowing how these forces influence the behaviour of the ball is related with the fact that the initial flight path can deviate, resulting in an unpredictable trajectory.

2.2.1. Boundary layer

Early research on the field have studied the flight of objects in vacuum until Prandtl (24) introduced the concept of a boundary layer, which corresponds to the volume of fluid between the object of study and the free stream fluid. The effects of friction, or viscosity, cause the adhesion of the fluid around the object to the surface, generating a gradient of velocity at the boundary layer, where the flow has the free stream speed, see Figure 5. At some point, due to the gradient of pressure in the front and rear surfaces of the ball, the boundary layer separates from the object having to possible states: laminar or turbulent.

In a laminar boundary layer the flow is nearly parallel to the surface and it will separate as soon as the flow speed is reduced. This generates in a gradient of pressure, which becomes constant after it separates, and it can be translated into a drag force that slows down the object, see Figure 6.
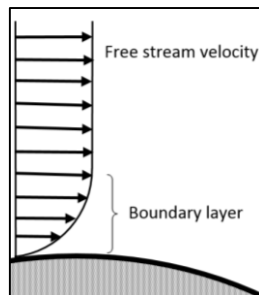
Figure 5. Boundary layer profile over a sphere for a viscous fluid.
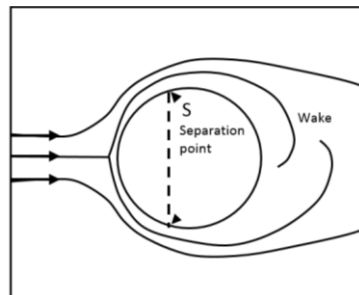
Figure 6. Laminar boundary layer separation on a sphere (adapted from Metha and Wood 1980).
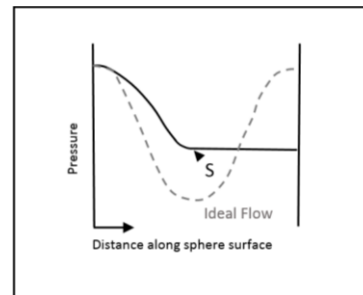
In a turbulent boundary layer, the fluctuations in velocity give a more chaotic appearance and it will delay the separation point to the back of the ball, generating a smaller gradient of pressure and therefore a lower drag force, see Figure 7.
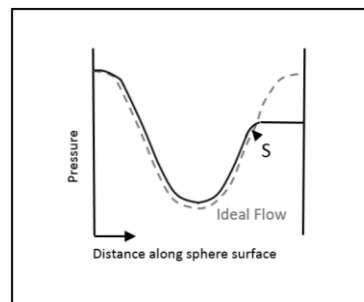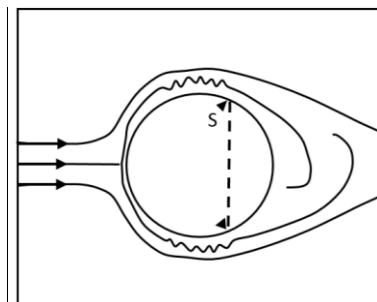
Figure 7. Turbulent boundary layer separation on a sphere (adapted from Metha and Wood 1980)

2.2.2. Reynolds number and Drag Crisis

The transition between the two states of boundary layer occurs if the Reynolds number, a dimensionless parameter which is a comparison between inertia forces and viscous forces, exceeds a critical value. The Reynolds number is defined by Equation 1.

$$Re = \frac{\rho \cdot v \cdot L}{\mu} = \frac{v \cdot L}{\nu} \tag{1}$$

Where:

- v is the mean velocity of the object relative to the fluid, in wind tunnel systems this is equal to the velocity of the flow, as the object is fixed in a support. (m/s)
- L is a characteristic dimension, in our case the diameter D of the ball. (m)
- μ is the dynamic viscosity of the fluid. (Pa·s or N·s/m² or kg/(m·s))
- ρ is the density of the fluid, air in this case. (kg/m³)
- ν is the cinematic viscosity of the fluid. (m²/s)

The previous research consulted, mostly from Metha (22), was focused on very different sports balls but similar research on Floorball balls could not be found. The data from other sports balls reveals that the critical Reynolds number values are between 10^4 and 10^5 where researchers have used wind tunnels and trajectory analysis to determine the aerodynamic coefficients experimentally.

The Figure 8 shows the Drag coefficient as a function of Reynolds number for different types of balls under no spinning conditions. The sudden reduction of the Drag coefficient, known as Drag Crisis, appears at the critical Reynolds number, establishing the transition from laminar to turbulent in the flow around the object. The graphic provides the evidence of the influence in the Drag crisis of roughness on the surface which occurs at lower speed if the surface is rougher, as in golf balls that are designed to travel farther and faster with the help of the dimples.
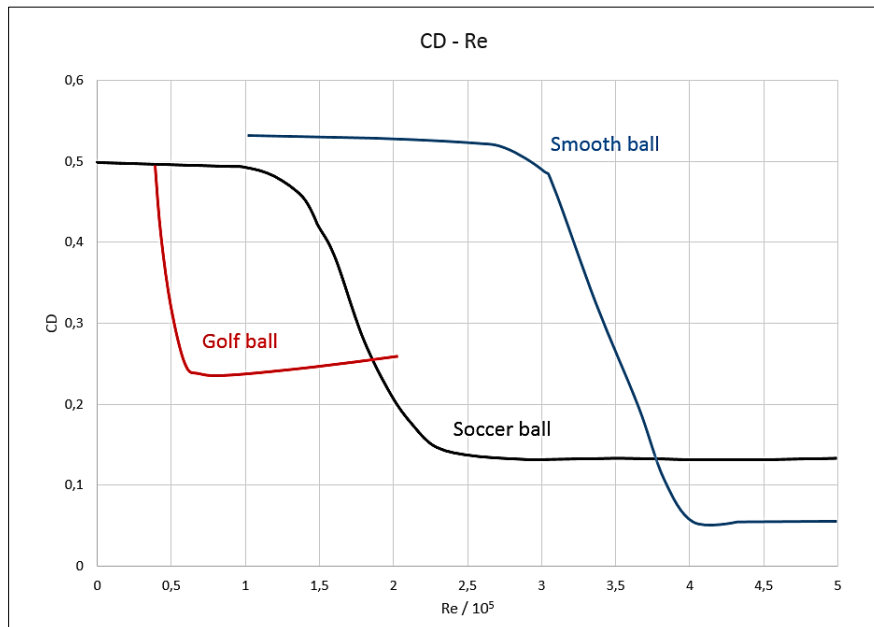
Figure 8. Drag coefficient as a function of Reynolds number

(adapted from Goff 2013)

2.2.3. Aerodynamic Forces and Coefficients

The flight of an object thought the air is influenced by the aerodynamic forces as a result of the viscosity of the fluid and the boundary layer conditions. Therefore, the two aerodynamic forces will be applying in the body, commonly known as Drag and Lift forces, Figure 9.

The drag force is by definition the force component in the opposite direction of the velocity, forcing the ball to slow down. The difference of pressure in the air flow surrounding a rotating ball is translated into a force, the Lift force, which is perpendicular to both the Drag force and the spin axis.
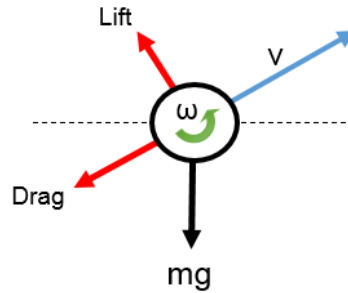
Figure 9. Forces applied in a spinning sphere

The Lift force direction can be up or down depending on the spin but it can also be sideways, when the spin of the ball is applied in another axis the lift forces are translated into a lateral force that deviates the straight trajectory, known as the Magnus effect. The trajectory of the ball will be influenced by those forces, which are normally calculated by means of Equation 2.

$$F_A = \frac{1}{2} C_A \rho A \mathrm{v}^2$$
(2)

Where:

- F_A is the corresponding aerodynamic force, Drag or Lift (N).
- C_A is the corresponding aerodynamic coefficient, Drag or Lift .
- ρ is the density of the fluid, air in this case (kg/m^3).
- v is the velocity of the object relative to the fluid (m/s).
- A is the reference area, m^2.

Though the wind tunnel experiments or simulations it is possible to determine the forces and calculate the coefficients, as the rest of the values are usually know. The coefficients are then calculated by means of Equation 3 and Equation 4.

$$C_D = \frac{2 \cdot F_D}{\rho \cdot \mathrm{v}^2 \cdot A}$$
(3)

$$C_L = \frac{2 \cdot F_L}{\rho \cdot \mathrm{v}^2 \cdot A}$$
(4)

The reference area depends on the geometry of the object, as it is the projected frontal area. In this case, the projected frontal area is the surface of a circle with the radius of the sphere, calculated by means of Equation 5.

$$A = \pi r^2$$
(5)

2.3. Aerodynamic Design Requirements

The information from previous research and manufacturers shows a tendency of aiming for a turbulent flow around the object that will lead to earlier Drag crisis, meaning that the ball can travel farther and faster though the fluid. This will be translated in the objective of having low drag values at the highest speed or Reynolds number.

The lift coefficient will maintain the ball in the air longer, as it usually opposes gravity, and therefore it is common to aim for higher lift values at lowest speeds or Reynolds number.

2.4. Computer Aided Design

The design of the improved products has been a major subject in the development of this thesis work, carried out in a Computer Aided Design environment by using the software Solidworks during the whole process. The basic floorball ball has been reproduced in a CAD model through some geometrical modifications. These new models include different features that of the ball that can influence its predictability and therefore need to be further studied. The main features modified in the ball can be distributed in the following categories:

- Dimpled pattern
- Holes distribution
- Modified holes

2.4.1. Basic Model

The present ball design has been studied as start point for the design of new products and then reproduced in the CAD Software, Figure 10. The distribution of the holes was done following the indications in SP document (10) in which it is also specified the nominal main dimensions: 72 mm of diameter and 10 mm diameter for the holes.

2.4.2. Dimpled Patterns

After the revision of the state of art regarding floorball equipment, it is clear that a major change introduced to the ball design is the dimpled surfaces. The specific geometry of the dimples has been modified to fulfil the weight requirements in a first revision and further modified to achieve better aerodynamic performance by an iterative process of calculations and modifications of the geometry. The shapes selected for the dimpled patterns have been round dimples, Figure 11, similar to those in the golf balls, and hexagonal dimples, Figure 12, looking for an innovative design. Besides the geometry of the dimples, the distribution of those makes differences in the aerodynamic behaviour, as shown with later versions of the models.
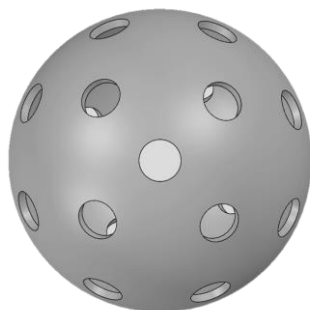
Figure 10. Basic model   Figure 11. Round dimples model   Figure 12. Hexagonal dimples model
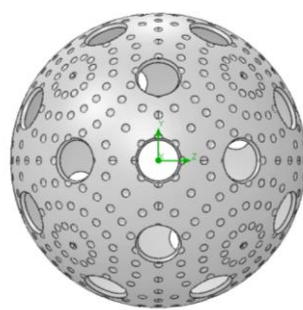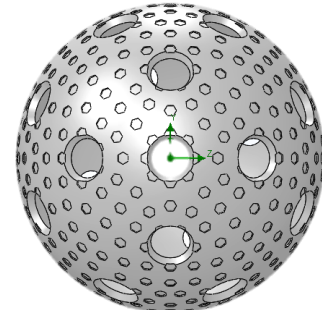
9

2.4.3.Distribution of Holes

The distribution of the holes of the ball is usually made following the design represented in SP document (10), which divides the ball in two equal halves, later joined to position a hole between two holes above the joint, see Figure 13.
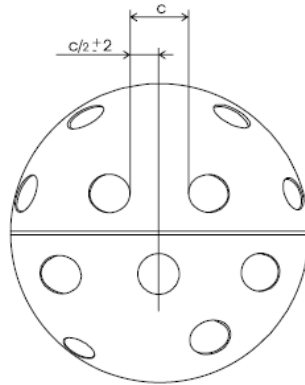
Figure 13. Position of the holes above the joint

from SP Technical Research Institute of Sweden

Regarding a more even distribution of holes, during the development of the design process the ball was divided into eight sections looking for symmetry in a higher number of axis. As each section should have the same number of holes, it leads to 3.25 holes that can be differently distributed in the named section. Due to the possibility of creating a seamless ball, the holes can be distributed along every direction as it is illustrated in Figure 14.

Distribution of Holes

SP Distribution	New Distribution
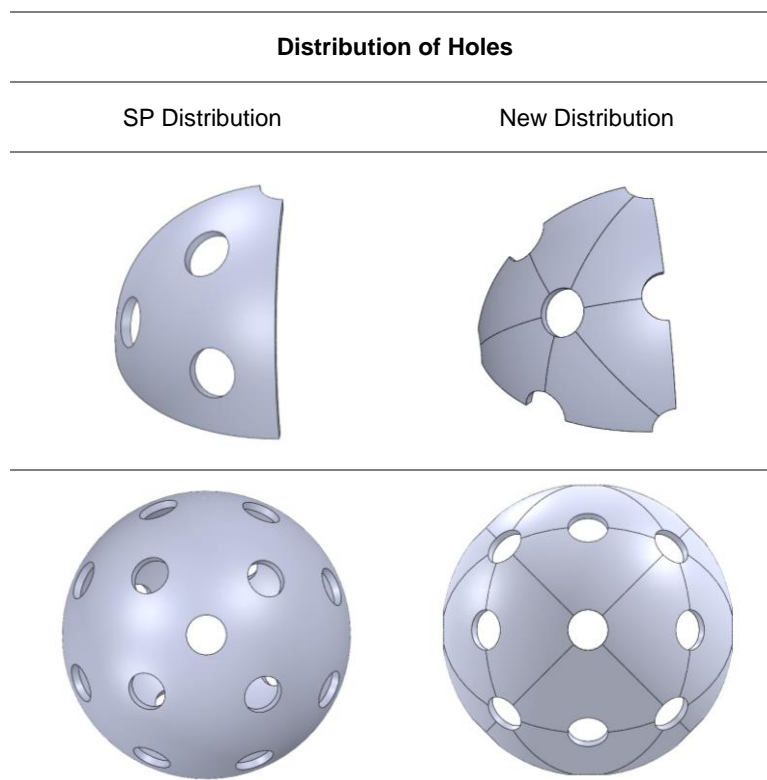
Figure 14. Distribution of holes, showing sections and complete balls.

2.4.4. Modified holes

The holes are unique feature of this sports ball, therefore they have been studied in order to find the design that leads to a better performance. Two main aspects of the holes studied were the dimension and the hole edge geometry.

- **Dimension**

As the requirements are defined as the diameter and allowed deviation, alternatives outside the tolerance margins have been studied to see the effects of this variation in the aerodynamic behaviour of the ball.

Two simulation models were created: one with smaller holes and one with bigger holes, both exceeding the tolerance margin by 1 mm. The aspect of the different models is shown in Table 2 comparing the design with normal diameter.

Dimension of holes		
Smaller Holes	Normal Holes	Bigger Holes
8 mm	10 ± 1 mm	12 mm

Table 2. Dimensions of holes

- **Geometry of the holes**

Most of the commercial balls have straight hole edges and generally they have not changed substantially in the latest designs of balls. However, the official competition ball has crater shaped holes claimed to give a better performance based on this additional feature. This has been the inspiration to reproduce different geometries of hole edges, in order to further study their influence on the flight of the ball. With this aim diverse models have been developed as shown in Table 3, showing various applications of chamfers on hole edges. The combination of both chamfers creates a new model whose shape reminds to the Venturi hole used in the concept of strangulation of the flow.

Geometry of the holes		
External Chamfer	Internal Chamfer	Venturi

Table 3. Details of geometry of the holes

3. Simulation

In order to evaluate the results, it was interesting to perform a dynamic computer aided simulation of the ball behaviour, with the aim of comparing the design possibilities outlined.

The simulation carried out in this study were basically a simulation of a wind tunnel in a 3D environment by using Flow Simulation in Solidworks. This software is a Computational Fluid Dynamics Software available in the same design software, which allows modifying the geometry or flow parameters in the same application. The ball models have been introduced in a computational domain, simulating the air flow interacting with the geometry.

3.1. Experimental Set up

The experiment input must be established as start point, to mimic the wind tunnel conditions. In this reproduction, all the models have been positioned equally with the fluid flowing along the x axis and the rotation, when applied, in the perpendicular z axis. The experimental set up for this simplified simulation allows to set some variables, the most relevant for this case of study are:

- Computational Domain Dimensions
- Velocity of fluid in different axis
- Velocity of rotation of the model
- Fluid
- Temperature and pressure

3.2. Simulation scenarios

Several scenarios were created by using the tool in the software called Parametric Study. This tool allows to modify variables and set objectives of the study. The data was recorded for each specific scenario providing the desired goal results for each Design Point.

The parametric study has been widely used while running the simulations of each model because the main interest of these experiments is to determine the Drag coefficient associated to a Reynolds Numbers. Two main scenarios were used to evaluate the drag coefficient in different situations. In the literature reviewed wind tunnel test in both Static and Spinning balls could be found, however it is common to begin with a static study. Despite this procedure is simplified, it allows to have a first idea of the behaviour of the object in the flow. Accordingly, a static study was carried out first in order to learn and discover the possibilities of the software. Secondly, looking for a more real scenario, a study with a spinning ball was performed for the most promising models. Finally, the results of both scenarios were used to compare the different ball geometry models and asses the best option.
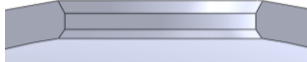
3.2.1. Static

In order to obtain graphical results to compare the models in the static study, the data from the simulations was collected in an Excel file, where the appropriate calculations are carried out for each model of ball. The range of speeds used was quite wide in a first approach to the tool, later reduced to represent more possible speed values for real game. The calculations were made from the force in the direction of the flow, or x direction. This force in the software is named as a Global Goal, which is lately named as the Drag Force for calculations.

3.2.2. Spin

The studies carried out with a spinning ball represent a more realistic behaviour of the models for real game conditions, as movements, translation and rotation will apply during the development of the game. Due to the rotational rate, it is interesting to calculate both Drag and Lift Forces, because the second is influenced by the rotation, therefore the two coefficients have been calculated.

As in the static study, the velocity of the flow has been adapted to a range of speeds applicable during game. The rotational rate was introduced in different values, however they were not selected necessarily to be relevant for the game. The calculations in this case have been made from the force in the direction

of the flow, or x direction, and the force in the perpendicular direction, or y direction. These forces in the software are named as a Global Goals with the addition of the direction x or y.

3.3. Results of Simulation

The results of the simulations carried out with Solidworks can be displayed in a great variety of systems and they can also provide visual support, both in static images and dynamic visualizations. For the present work, it was chosen to record the outcomes mainly in numerical results and some graphical results to have a visual approximation to the sphere-flow interaction.

Regarding the graphical results, there are numerous options to customize the variables and plot the desired results for specific parameters of the flow. For instance, the streamline plotting option was used, Figure 15, since it gave a similar visualization as a real wind tunnel test.
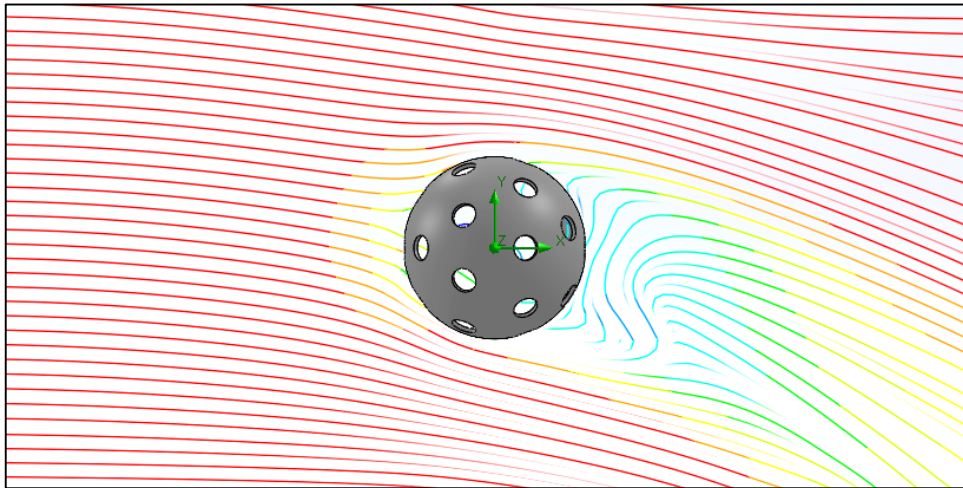
Figure 15. Streamlines representation on Spinning ball Simulation

In some particular designs, it was found useful to study a dynamic simulation of the flow in order to have detailed idea of the passing flow through the holes of the ball.

4. Evaluation of Design

4.1. Evaluation Method

During the development of this thesis work, different evaluations have been performed on the designed geometries, leading to an iterative process consisting of evaluation of drag coefficient results and redesign, as the Figure 16 describes.
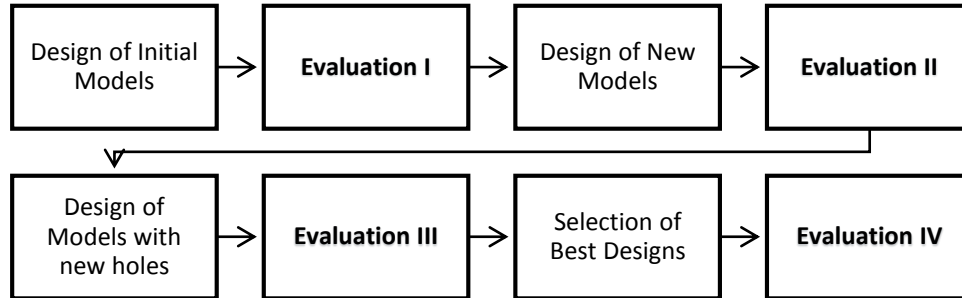
Figure 16. Evaluation and Redesign Process

In most of the evaluation stages, the reduction of drag coefficient was the main criteria for the selection of the best alternatives. The following sections will describe the geometries and simulations applied in each case, then concluding with general results.

4.2. Evaluation I

The first models of balls designed had variations only regarding the aspect of the surface, being smooth or with a dimpled surface. Different shapes of dimples were used, the geometries included hexagonal and round dimpled patterns. Also, two different distribution of holes were tested in a first step of evaluation. All the configurations used for this first evaluation are shown in the Figure 17.
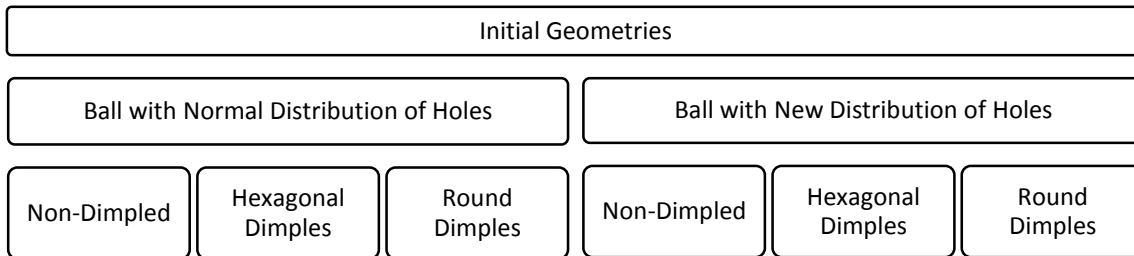
Figure 17. Geometries for Evaluation I

These geometries were then modified to adjust the mass criteria by using the *Design Study* tool from Solidworks, which allows to set the mass as an objective and dimensions in the model as variables. The main dimensions modified are the depth and width of the dimples, and the modifications provided an extensive variety of models. The following Table 4 from the software shows the Design Study applied to the Hexagonal Dimpled Ball. Similar operations have been carried out with the round dimpled balls. Setting a range of values for the dimples depth and width obtained several combinations that fulfil the mass requirement, being between 22 and 24 grams.

		Current	Initial	Optimal (0)	Scenario 1	Scenario 2	Scenario 3	Scenario 4	Scenario 5	Scenario 6
Dimples Depth		0.5mm	0.5mm	0.5mm	0.5mm	0.4mm	0.5mm	0.45mm	0.5mm	0.45mm
Dimples Width		2mm	2mm	2mm	3mm	2.5mm	2mm	2mm	1.25mm	1mm
Mass2	(22 g ~ 24 g)	22.9979 g	22.9979 g	22.9979 g	22.1535 g	22.874 g	22.9979 g	23.0773 g	23.3778 g	23.4853 g
Mass1	Is exactly 0.023	22.9979 g	22.9979 g	22.9979 g	22.1535 g	22.874 g	22.9979 g	23.0773 g	23.3778 g	23.4853 g

Table 4. Design Study from Solidworks applied to Hexagonal Dimpled Ball.

Once the configurations were selected with the appropriate mass, the simulation started and the Parametric Study was set for a No Spin test.

14

A wide range of velocities in the x direction were selected in order to have a broad vision of the behaviour of the models. The speed was reduced progressively to focus the attention on the game speed range, thus it was more relevant for the aim of the project.

Again for the hexagonal dimples as the main example, the configurations were simulated leading to the values of Drag Coefficient shown in Figure 18 and Table 5, where the configurations C6 and C7 showed the lowest values.
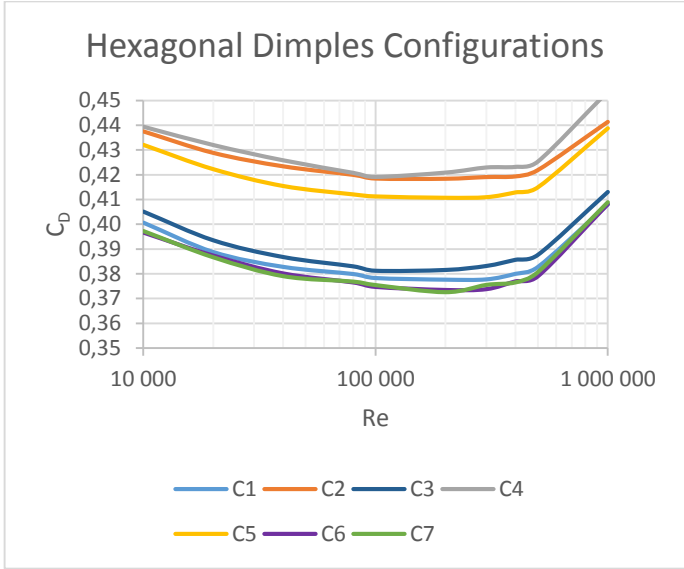
Figure 18. Drag coefficient plotted as a function of Reynolds number for Hexagonal dimples

Hexagonal Dimples Ball							
Thickness (mm)	1.75						
Configuration	1	2	3	4	5	6	7
Weight (g)	22,874	22,9979	23,0773	23,3778	23,4853	23,121	23,2441
Dimples Depth (mm)	0,4	0,5	0,45	0,50	0,45	0,3	0,25
Dimples Width (mm)	2,5	2	2	1,25	1	2,5	2,5
Re	C_D	C_D	C_D	C_D	C_D	C_D	C_D
1E+04	0,401	0,438	0,405	0,439	0,432	0,397	0,397
2E+04	0,389	0,429	0,394	0,432	0,422	0,387	0,387
4E+04	0,383	0,423	0,387	0,426	0,415	0,380	0,379
8E+04	0,380	0,420	0,383	0,421	0,412	0,376	0,377
1E+05	0,378	0,418	0,381	0,419	0,411	0,375	0,375
2E+05	0,378	0,418	0,382	0,421	0,411	0,373	0,373
3E+05	0,378	0,419	0,383	0,423	0,411	0,374	0,376
4E+05	0,380	0,419	0,386	0,423	0,413	0,377	0,377
5E+05	0,383	0,422	0,388	0,425	0,415	0,379	0,381
1E+06	0,408	0,441	0,413	0,454	0,439	0,408	0,409

Table 5. Drag coefficient for different Hexagonal Dimples

The results obtained from this first stage of evaluation were based on the comparison of the drag coefficient between the traditional ball design and the new developed models, choosing for each type of dimples the best configurations.

Consequently the graphics, Figure 19 and Figure 20, show the Drag coefficient plotted for several Reynolds numbers, where the light blue colour corresponds to the traditional ball design. In the graphics, the acronym ND stands for New Distribution of holes.
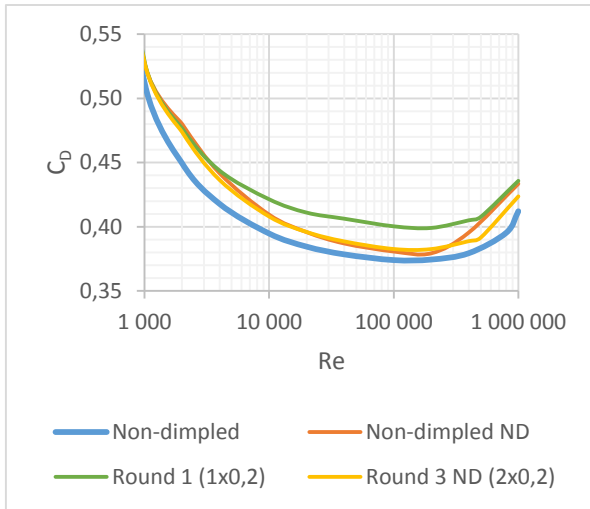
Figure 19. Drag Coefficient as a function of Reynolds Number for Round Dimpled Balls
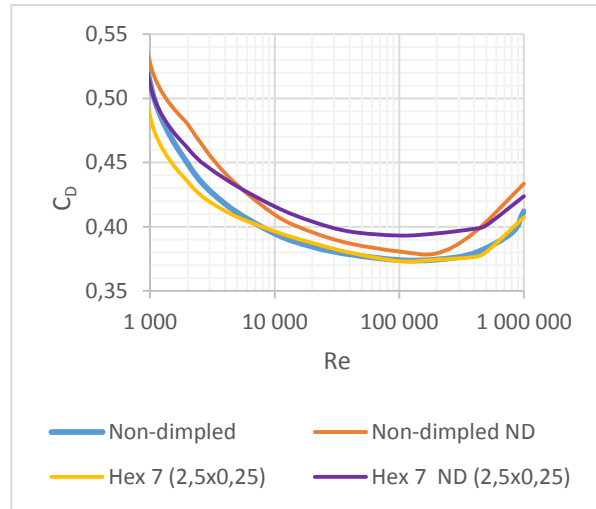
Figure 20. Drag coefficient as a function of Reynolds Number for Hexagonal Dimpled Balls

An important general conclusion was that a great part of the geometries studied did not improve the aerodynamic coefficients, compared to the traditional design of the ball. Looking at geometry Hex 7 in Figure 20, it can be noted that the drag coefficient was reduced at low speeds, at a Re below 10.000 corresponding to a speed below 2,1 m/s. Above this speed, Hex 7 behaved similarly to the non-dimpled ball, thus the conclusion of the first evaluation was that the dimpled configurations likely cannot make an appreciable improvement of the predictability of the ball.

4.3. Evaluation II

Since the previous evaluation did not give any concluding results, the simulations were carried out on new geometries. The geometries chosen for this next evaluation were divided in the following categories: Dimples and holes. The name and number of these new geometries are shown in the image below, Figure 21.
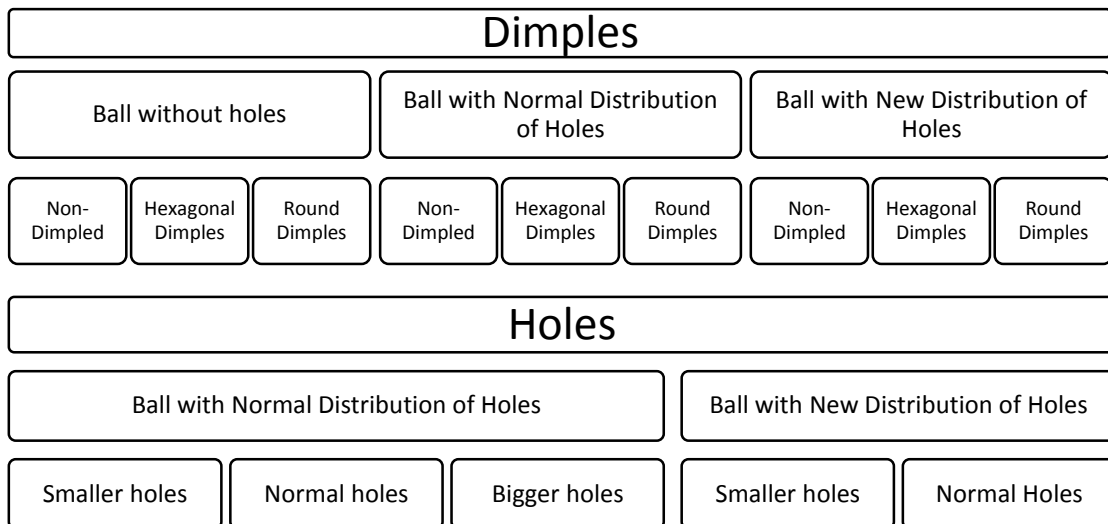
Figure 21. Geometries organized in categories: Dimples and Holes.

The simulation of the geometries was done by using the Parametric Study with a wide range of velocities in the x direction, though the results have been studied in a more suitable range of speeds for the game. Also here, the parametric study was set for a No Spin test.

The simulation results for dimples influence are shown in Figure 22, for non-hollowed spheres. It seems that the drag coefficient for the dimpled spheres is meaning that they generate more resistance to air flow. Only for Reynolds numbers below 1 a lower drag is achieved for the Hexagonal Dimpled sphere, which is not really relevant because it corresponds to very low speeds.

For the hollowed geometries, comparing both distributions of holes, normal distribution and new distribution (ND), similar tendencies to the non-hollowed balls were seen, indicating that these geometries and patterns in Figure 23 did not significantly improve the aerodynamic drag resistance.
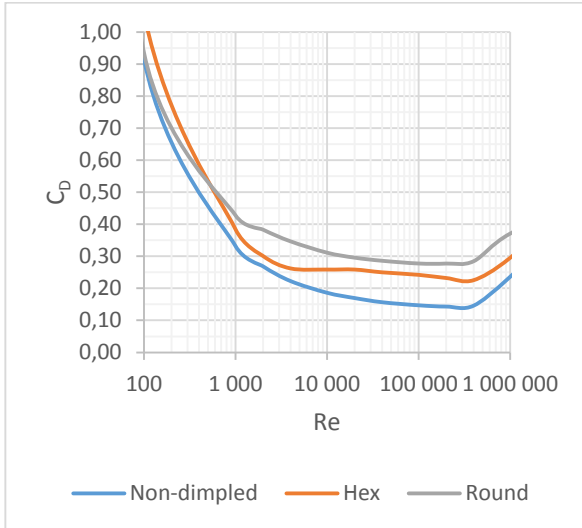
Figure 22. Dimples influence on spherical surfaces.
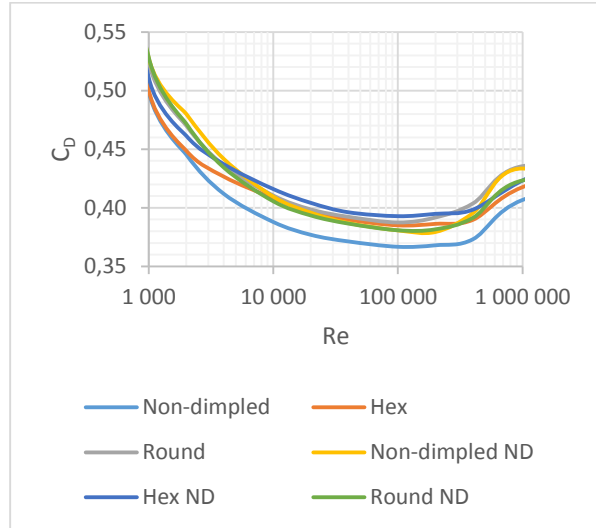
Figure 23. Dimples influence on hollowed balls

The new distribution of holes (seamless ball geometry) was compared with the traditional distribution. The results showed that the simulated drag coefficient was higher for the seamless geometry than for the traditional distribution. The new distribution only reduces the drag at very low speeds, around 0,0021 m/s, or very high speeds, from 205 m/s, the higher speed considered not to be possible in a Floorball game situation.

For further work, the diameter of the holes was allowed to exceed the tolerance margins given by the current rules in order to study the influence on the drag coefficient, see Figure 25. The results showed that the smaller the holes, the lower drag was generated so the ball maintained the speed for longer and faster trajectories. Larger holes made the ball slower, generating more resistance to the air flow.
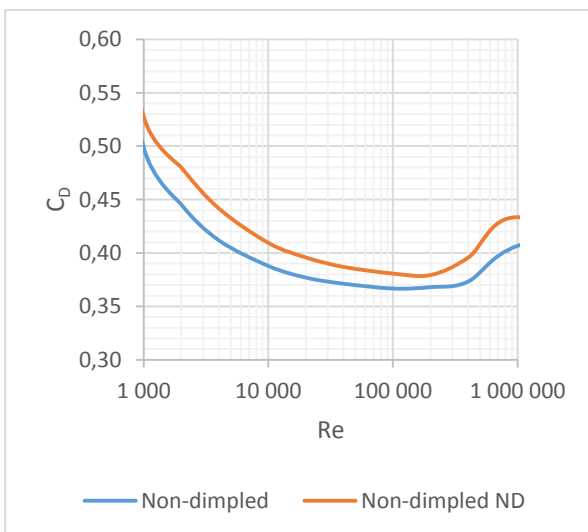
Figure 24. Distribution of holes influence on drag coeffiecient
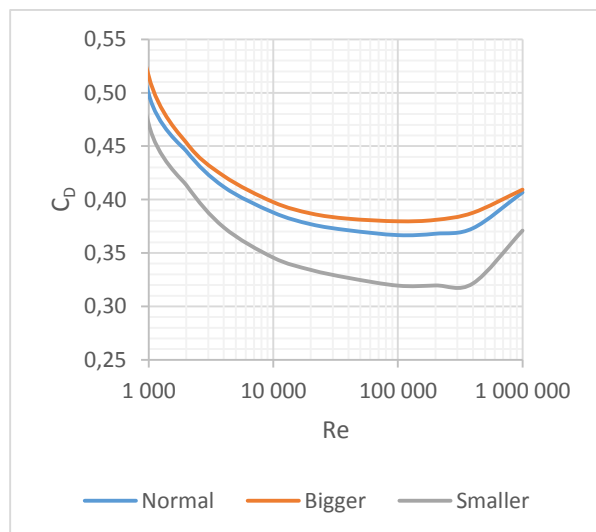
Figure 25. Dimension of holes influence on drag coefficient

4.4. Evaluation III

Further simulations were carried out again in the No-spin simulation scenario. In this case, the velocities applied in the x direction have been reduced to the range of 10 to 40 m/s, which is more relevant for the speeds during the game. The following Figure 26 shows all the interesting geometries at this stage of the work. It can be seen that four out of six alternatives studied could reduce the drag coefficient. For the better four out of the six hole geometries, there were two possible to draw.

The most obvious result was that the smaller holes reduces the drag considerably. Important here is that such small holes do not fulfil the requirements of IFF, as the holes have a diameter (8 mm), which is 1 mm less than currently allowed.
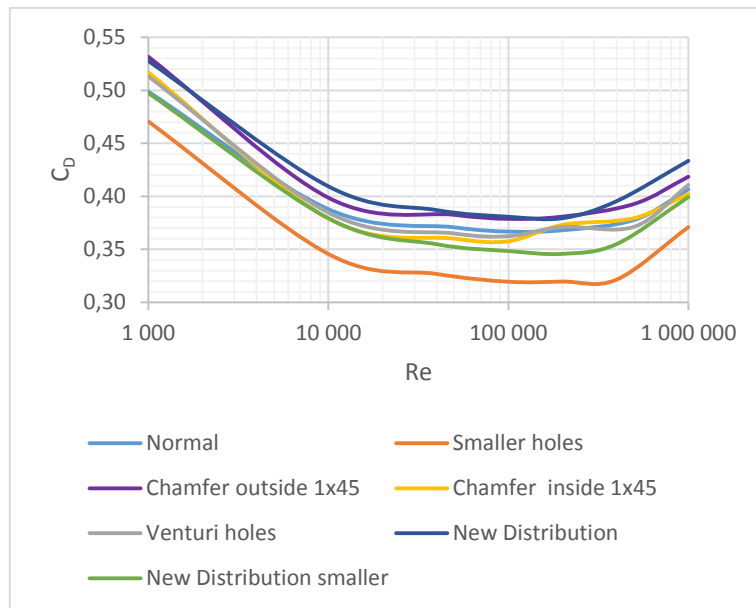
Figure 26.Drag coefficient plotted as a function of Reynolds number for all the geometries

The geometries with an inside chamfer design or with a venturi design may give lower drag than the straight hole edges in the original design. This is clearly seen in Figure 27, where the drag coefficient is plotted against the speed in m/s. Here, a drag reduction is seen for a velocity lower than 30 m/s, which is a reasonable speed for the ball during play. The low drag geometry of holes edge with internal chamfer was included for a Swedish Patent application, (25) .
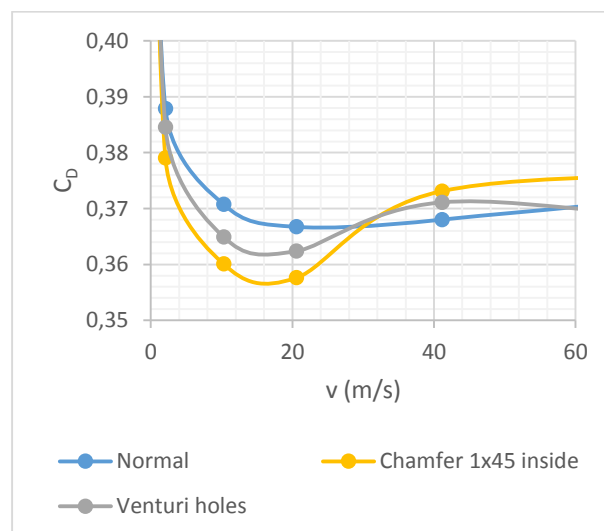
Figure 27. Drag coefficient as a function of speed in m/s

4.5. Evaluation IV

The results from Evaluation III have indicated some interesting results on improvements of the ball geometry. It should be pointed out that the results represent static simulations by estimated values of the real coefficients. Therefore to continue with the aerodynamic evaluation of the design, the literature was reviewed again focusing on the influence of the rotation in sports balls. As the spinning of the ball can cause deviations on the trajectory due to the Magnus effect, a spinning simulation was done to study this phenomena and also the drag for spinning balls.

The simulations of both static and spinning were carried out for the most promising geometries and also for some combinations. The geometries analysed are shown in the Figure 28 below.

Geometries		
Ball with Normal Distribution of Holes		Ball with New Distribution of Holes

Normal holes	Smaller holes	Chamfer inside 1x45	Venturi Holes	Hexagonal Dimples	Hexagonal dimples with Chamfer Inside	Smaller holes	Normal Holes
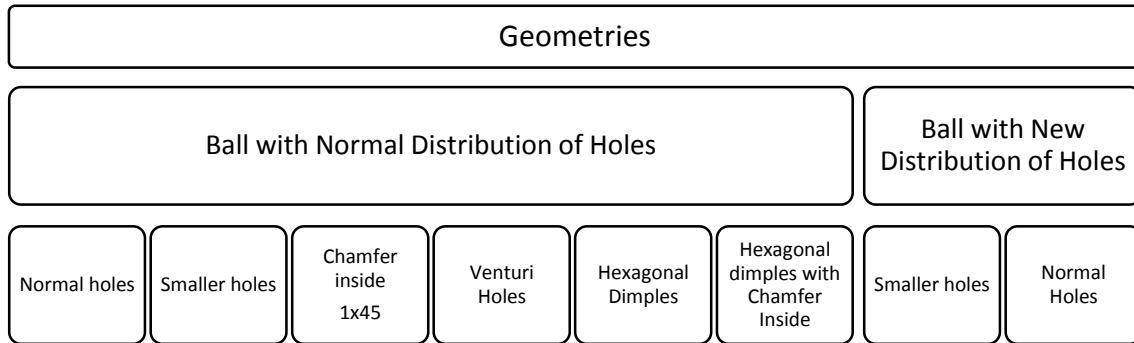
Figure 28. Geometries for Evaluation IV

4.5.1. Static ball simulation of adjusted geometries

The simulations performed were chosen to correspond to velocities between 0,2 and 205 m/s. The resulting drag coefficients are shown in Figure 29 and Figure 30, divided into two categories depending on the drag coefficient. The geometries that gave a higher drag coefficient than the traditional geometry were not studied further.
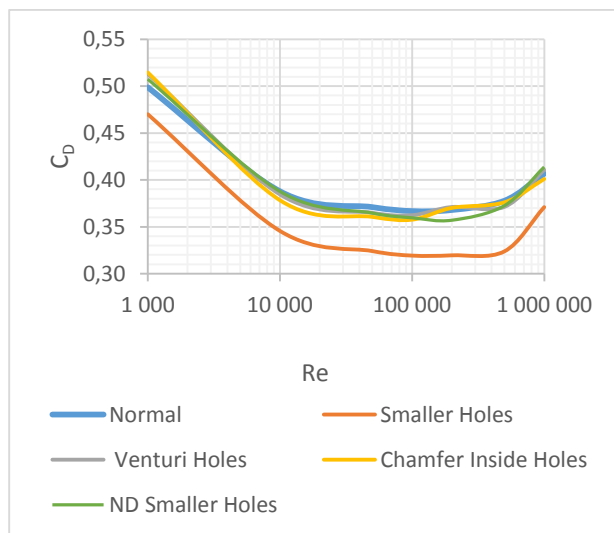
Figure 29. Drag coefficient as a function of Reynolds Number for geometries with lower drag
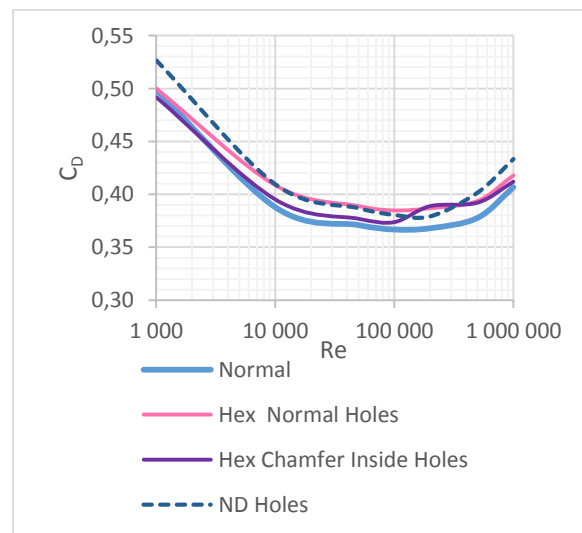
Figure 30. Drag coefficient as a function of Reynolds Number for geometries with higher drag

Regarding the geometries resulting in a relatively low drag coefficient, it is clear that the smaller holes have the largest influence, as seen in Figure 29. For the rest of the geometries in Figure 29, the data was analysed in detail to determine the most promising alternatives. The design with both a new distribution and smaller holes has clearly a lower drag than traditional design would likely be interesting for a good range of speed.

Comparing the other two geometries, both allowed by current rules, the holes with a chamfer inside indicated a lower drag for speed below 34 m/s, while at higher velocities the drag increases to the levels of the normal ball. The results in Figure 31 are also given in Table 6.

19
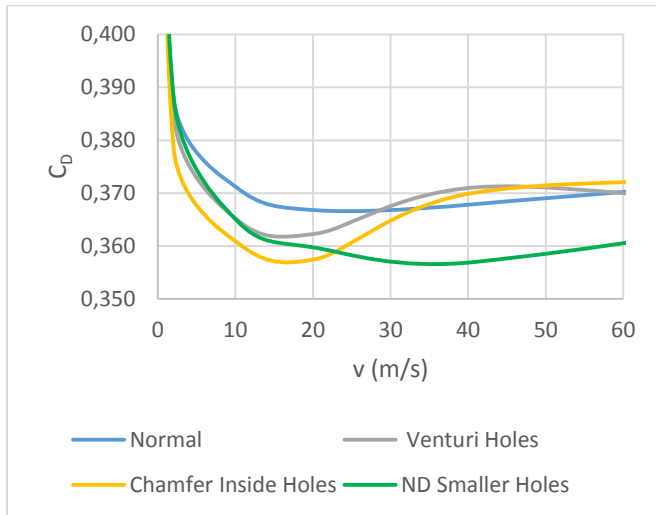
Figure 31. Drag coefficient as a function of speed in m/s for the mosot promising models.

Re	V (m/s)	Normal	Venturi Holes	Chamfer Inside	ND Smaller Holes
		C_D	C_D	C_D	C_D
1E+03	0,206	0,499	0,513	0,515	0,507
1E+04	2,056	0,388	0,385	0,378	0,388
5E+04	10,280	0,371	0,365	0,361	0,365
1E+05	20,556	0,367	0,362	0,358	0,360
2E+05	41,111	0,368	0,371	0,370	0,357
5E+05	102,780	0,378	0,371	0,376	0,373
1E+06	205,556	0,407	0,411	0,401	0,414

Table 6. Drag coefficient for most promising geometries as in Figure 31.

4.5.2. Rotating ball test

In order to further improve the simulations aiming to better represent real game conditions, a rotating ball simulation was carried out. Here, the rotational speed in the z direction was set to a few different values to analyse the influence of the rotation rate. The chosen rotation rate values were 5, 25, 50 and 100 rad/s. For the translation velocity (in the x direction), the values were kept at reasonable game speeds such as 2, 10, 20 and 30 m/s.

At the low rotational rate of 5 rad/s, the drag was close to that from the static test where the lowest drag was seen for the smaller holes. Moreover, all the studied geometries had the highest drag at the lowest translational speed (2m/s), as shown in Figure 32.

In this study two additional models were included, the hexagonal dimples with normal holes and the hexagonal dimples with chamfer inside holes, and both resulting in lower drag coefficient than in the static test. This shows the influence of dimples with a spinning ball but still the smaller holes and the inside chamfer in different combinations are interesting.
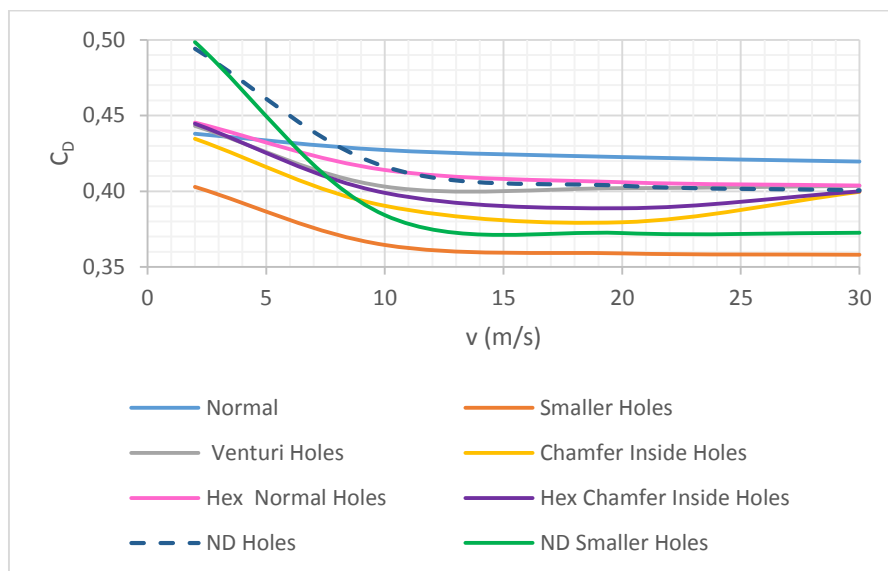
Figure 32. Drag coefficient as a function of speed in m/s for different geometries at w of 5 rad/s

The next rotational speed applied was 25 rad/s, represented in Figure 33 and Figure 34, showing that the global results are quite similar to the 5 rad/s: the smaller holes are the better option for a wide range of translational speeds. The new distribution of holes generates an increase of the drag coefficient from 4 m/s until 17 m/s where the drag was reduced. For the other geometries represented in Figure 34, a

relative reduction of drag was observed below 10 m/s, while above this value they behaved similarly to the ball with the traditional design. The evaluation of the geometries at the rate of 50 rad/s resulted in similar outcomes as for 25 rad/s and are not shown here.

Figure 33. Drag coefficient as a function of speed in m/s for different geometries at w of 25 rad/s.
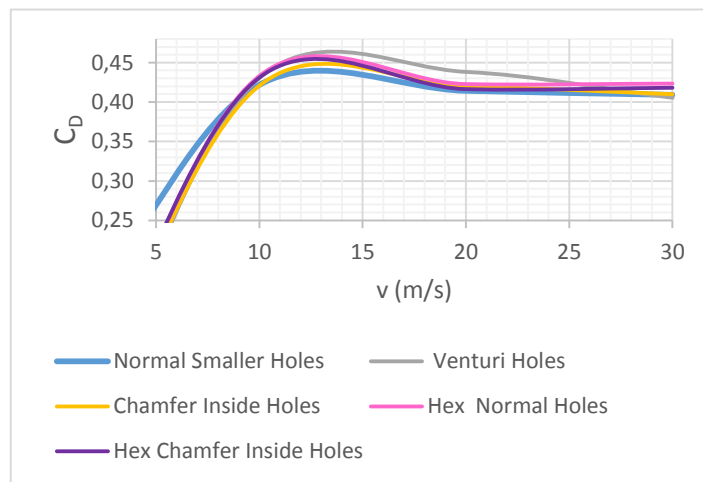
Figure 34. Drag coefficient as a function of speed in m/s for different geometries at w of 25 rad/s.

A summary of drag reduction with the geometries studied, compared with the traditional geometry, is shown in Table 7. The geometries with chamfered holes showed a similar performance as the normal ball above 10 m/s, but below 10 m/s the drag was lower. Again, the new distribution of holes did not contribute to the reduction of the drag coefficient.

w (rad/s)	v (m/s)	Smaller holes	Venturi Holes	Chamfer inside	Hex dimples	Hex chamfer	ND	ND Smaller
25	2	-4%	81%	69%	65%	63%	25%	23%
	10	10%	-2%	0%	-3%	-2%	-14%	-14%
	20	13%	-6%	-1%	-2%	-1%	-4%	5%
	30	14%	1%	0%	-3%	-2%	-1%	6%
50	2	-22%	-14%	5%	8%	6%	-17%	-10%
	10	2%	-1%	6%	-1%	4%	-12%	-22%
	20	10%	-2%	1%	-3%	-3%	-14%	-12%
	30	4%	-5%	-1%	-3%	-3%	-10%	-4%

Table 7. Drag reduction given in percentage, compared to the traditional model, at rotational rates of 25 and 50 rad/s

In the last simulation, at the rotational rate of 100 rad/s, the behaviour of the designs was completely changed. The ball with smaller holes had higher drag than the other geometries, also interesting to observe that the hex dimpled and chamfer designs had lower drag generally, shown in Figure 35 and Figure 36.

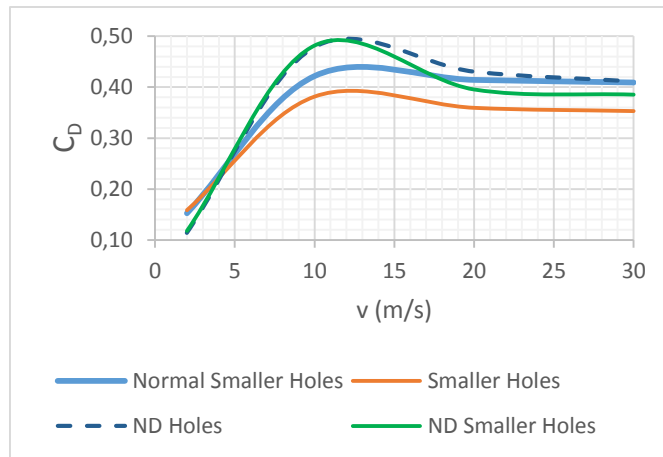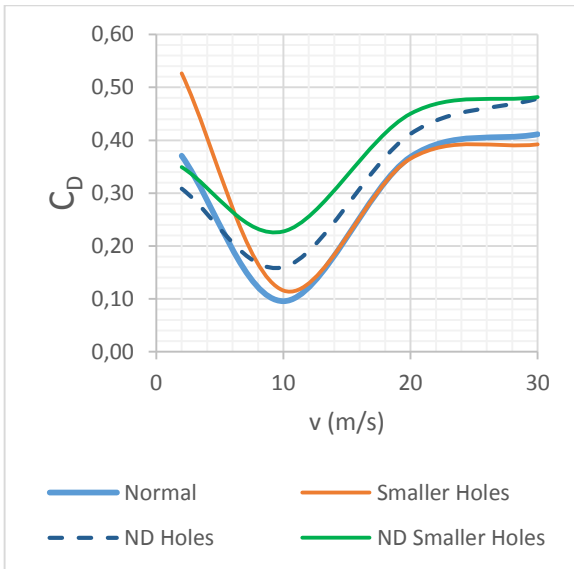Figure 35. Drag coefficient as a function of speed in m/s for different geometries at w of 100 rad/s
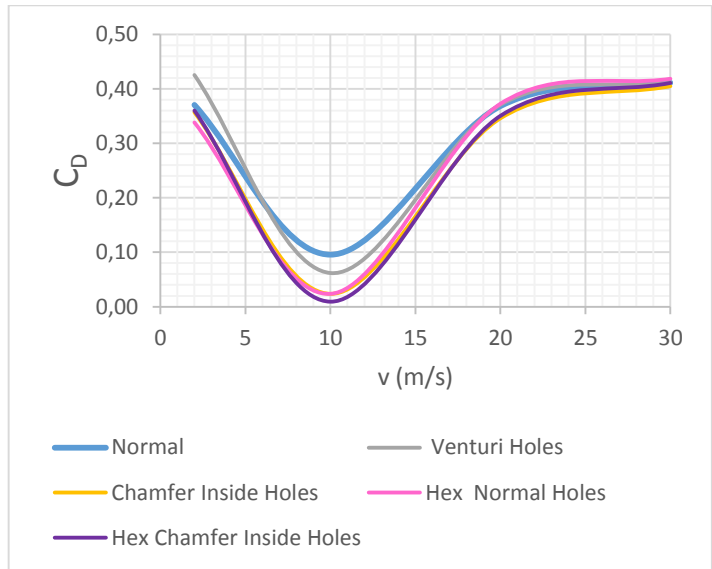
Figure 36. Drag coefficient as a function of speed in m/s for different geometries at w of 100 rad/s

Also the Lift coefficient, described in Section 2.2.3, was simulated at low Reynolds number, more specifically at a translational speed of 2 m/s and at different rotational rates. The graphics on Figure 37 and Figure 38 show the results on behaviour for the geometries given before.

The highest lift values was simulated for the smaller holes geometry, followed by the Venturi geometry and the new distribution of holes with smaller diameter. The other geometries gave similar Lift coefficient as the traditional ball.
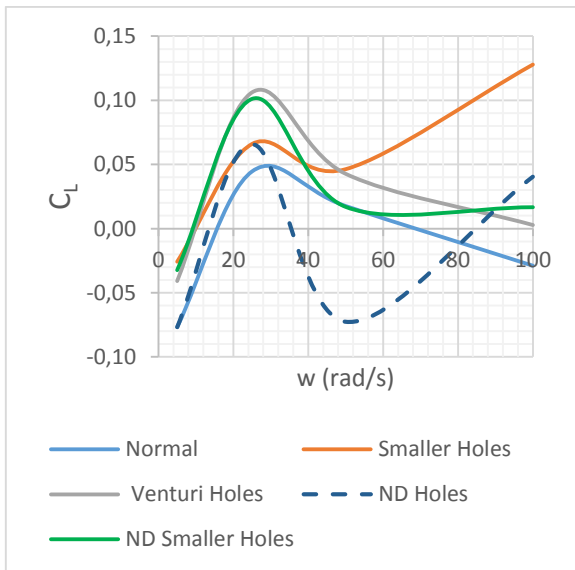
Figure 37. Lift coefficient as a function of the rotational rate [rad/s]
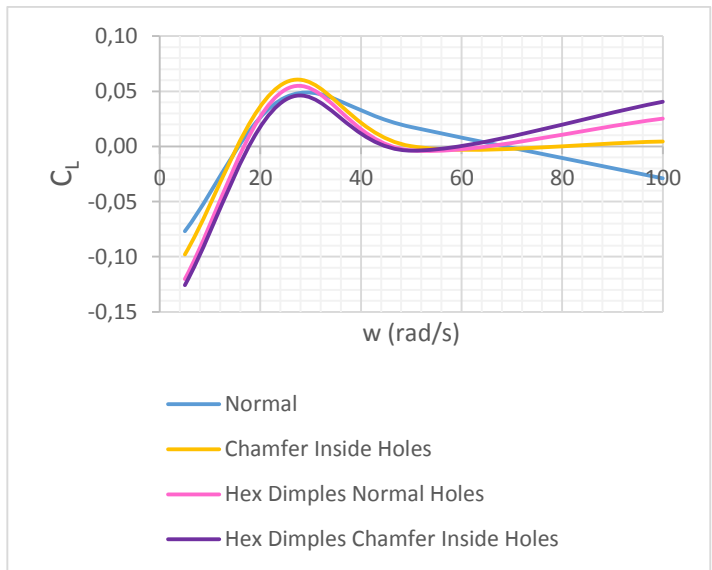
Figure 38. Lift coefficient as a function of the rotational rate [rad/s]

The results from simulations of Lift Coefficient supported the previous interest in further work with smaller holes, based on an increased lift coefficient added to a reduced drag coefficient, by that supporting expectations on longer and faster ball trajectory. The chamfer holes geometry was indicated to reduce the drag for some combinations of rotation and translational speed and in some others they behave similar to a normal ball. The new distribution of holes did not contribute to a reduction of drag coefficient in itself, since the drag reduction was seen always related also to smaller holes.

4.6. Conclusions drawn from simulations of drag and lift

The simulations of the influence of various geometries resulted in the following conclusions:

- Dimpled surfaces did not improve the aerodynamic behaviour and consequently the predictability of the ball. Moreover, the new distribution of holes did not reduce the drag.

- Smaller holes than the allowed by regulation may reduce the drag considerably while the dimpled patterns are likely not well designed. A drag reduction can be achieved by changing the hole edges and maintaining the holes dimension, which provides several variables in the ball geometry allowed by current rules.

- Smaller holes were indicated to reduce the drag coefficient by about a 10% compared to the current ball design, while changing the hole edges to Venturi or Chamfer inside reduced the drag by about 2%.

- Simulations of the spinning ball indicated that smaller holes would provide further drag reduction and increased lift. Chamfered hole edges may reduce the drag for some combinations of rotation and translational speed, but for some other combinations the behaviour was similar to a normal ball.

5. Materials and Manufacturing

5.1. Material Properties

Floorball balls are generally made of a thermoplastic polymer. Polyethylene is commonly used as in many other applications that require inexpensive durable and light weight components. In general, injection moulding grades are preferred, as an adaptation to the prevailing manufacturing processes.

5.1.1. Material Properties of Polyethylene

The term polyethylene relates to a variety of thermoplastics, widely used for injection moulded as it has the advantage of low costs when mass produced and it has good recyclability. Moreover, the products manufactured with polyethylene usually have a good impact strength and flexibility. Table 8 summarizes the typical properties of polyethylene, as it is common to have different densities for this polymer depending on the characteristics of the desired product.

Material Properties		
Density	0,924	g/cm^3
Mechanical Properties		
Tensile Modulus	450-1500	N/mm^2
Tensile strength	10-43	N/mm^2
Elongation at break	100-500	%
Flexural Modulus	280-4400	N/mm^2
Notched Impact strength (23°C)	2-80.1	kJ/m^2
Shore D - hardness	55-76	
Thermal Properties		
Melting point	121-137	°C

Table 8. General Properties of Polyethylene

5.1.2. Materials for Additive Manufacturing

Additive Manufacturing technology allows for creating complex geometries at low costs and short processing time. Nevertheless, among the limitations, the materials available are not as many as in traditional plastic manufacturing processes such as for injection moulding.

Although AM allows to process materials of almost all types, the variety available of processes is limited but grows continually by both process development and material research, mostly done by the machine manufacturers who exclusively sell the specific material for their products.

Focusing on Floorball balls, the challenge was to find a material, among the polymers available for AM processes, which could behave as similar as possible to the ones made of polyethylene by injection moulding. The variety of available polymers for AM are in general quite limited. The current AM process are generally limited to a few grades in some cases also to some shapes such as filaments or powder.

Fused Deposition Modelling, or commonly known as 3D printing, is based on the extrusion of thin fibres, therefore the raw material need to be in the shape of a filament that melts at relative low temperatures. Considering the main manufacturers of such machines, the available filaments can be found made of Acrylonitrile butadiene styrene (ABS), Polylactic acid (PLA) and Polyamides

Selective Laser Sintering, a process based on the melting and re-solidifying of a plastic particle layer, works with powder as raw material and in this case polyamides are a suitable candidate. These polyamides for SLS differ from the ones used in plastic injection moulding mainly because of the process characteristics: locally molten at atmospheric pressure versus completely molten and pressure injected, but also because of the specific polyamide used.

Other AM techniques, like Freeformer, introduced by the company Arburg (19), allows to use standard granulates, which opens a wide range of possibilities regarding the materials for AM. By using this specific process, it would be possible to shape products in Polyethylene so it would be the ideal process to manufacture functional prototypes or even future floorball balls in a commercial scale.

5.2. **Manufacturing Process**

After the visit to Elmia Polymer Fair and research on companies in the area of Gothenburg, the contact with some companies specialised in additive manufacturing techniques and development of prototypes was stablished. The requirements of the developed products were presented with the suggestion of manufacturing the ball with a flexible, stiff and durable material that could behave like the polyethylene injected balls.

The suggestions given for stated demands were mainly that the available process would be Selective Laser Sintering, due to the better mechanical properties it can offer when combined with polyamide powder. The process does not require any base or support as the powder around the sintered part will stabilize it during the process. The chamber is filled with powder, about 50µm grain size, and a laser beam will generate the contour by locally melted particles, which solidify by thermal conductivity. The chamber is mounted on a piston system in order to adjust the layer thickness once the laser finishes melting a layer. The chamber is then filled with powder again and the process continues with the next layer until the whole part is completed.

5.3. **Manufacturing of Prototypes**

The manufactured prototypes had the chamfer feature inside the holes as it was preferred from the simulation results while maintaining the diameter of the holes, by that within the current certification limits.

Prototypes were been manufactured by Prototal PDS AB using the Selective Laser Sintering process. The material for the prototypes was a polyamide with the commercial name PA 2200, having characteristics summarized in Table 9. The technical data of the sintering machine is provided by the company and shown in Table 10.

Material Properties			
Average grain size	Laser diffraction	60	µm
Bulk Density	DIN 53466	0,435-0,445	g/cm^3
Density of Laser-sintered part	EOS method	0,9-0,95	g/cm^3
Mechanical Properties			
Tensile Modulus	DIN EN ISO 527	1700±150	N/mm^2
Tensile strength	DIN EN ISO 527	45±3	N/mm^2
Elongation at break	DIN EN ISO 527	20±5	%
Flexural Modulus	DIN EN ISO 178	1240±130	N/mm^2
Charpy – Impact strength	DIN EN ISO 179	53±3,8	kJ/m^2
Shore D - hardness	DIN 53505	75±2	
Thermal properties			
Melting point	DIN 53736	172-180	℃

Table 9. Material properties of PA2200 from the manufacturer EOS.

Sintering machine	
Machine Manufacturer	EOS
Machine Model	Formiga P100
Material	PA2200
Layer Thickness	0.10 mm

Table 10. Sintering machine information

6. Evaluation of Prototypes

The manufactured prototypes were evaluated in order to assess the improvements achieved by the developed design and compare them with the existing precision balls. The assessment included a verification of the size requirements and an analysis of the aerodynamic performance of the ball. The evaluation of the balls was done in collaboration with Chalmers Sports and Technology group and with of two Innebandy clubs in the area of Gothenburg.

6.1. Requirements

The requirements are based on applicable standards which have been collected in the document "Material Regulations Certification Rules for IFF-marking of Floorball Equipment SPCR 011" (9) published by the official certification agency SP Technical Research Institute of Sweden. The procedure to follow during certification and the requirements on the testing equipment are explained in this publication. The current rules for the ball are summarized in Table 11.

Weight	23 ± 1 gr	**Surface Fineness**	Ra 1—5 μm
Diameter	72 ± 1 mm	**Number of Holes**	26
Diameter of holes	10 ± 1 mm	**Breaking stress**	6.0 N/mm^2
Hole's internal placement over joint	c/2 ± 2 mm	**Rebound**	650 ± 50 mm

Table 11. Requirements for certification

The measurement of weight, dimensions and surface fineness was performed at Materials and Manufacturing Technology Department in Chalmers as described in section 6.2.

Regarding the rules for breaking stress and rebound, it was decided that these were not applicable, due to their dependence on the material properties. The material chosen for the prototype was polyamide that would make the ball very different compared to polyethylene behaviour.

6.2. Dimensional tests

6.2.1. Weight

The prototypes were weighted in a precision scale with accuracy of 0,0001 grams. The pictures show the results achieved for two versions of prototypes, the difference being mainly the thickness of the wall.

6.2.2. Dimensional measurements

The measurement of external diameter and hole diameter was performed by using a sliding calliper with electronic screen and 0,01 mm precision. Both measurements were repeated five times, as specified in the SPCR 011 (26). The position of the holes has not been measured as the ball is manufactured with a seamless procedure and therefore the holes were positioned during the geometrical design of the prototypes.
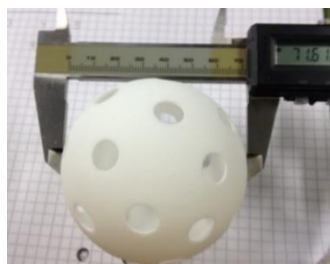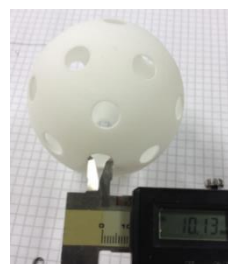

Figure 39. Measurement of the diameter   Figure 40. Measurement of hole diameter

6.2.3.Surface Fineness

The surface of the prototypes was analysed by using a stylus device, Figure 41. The procedure followed gives an approximate approach to the real surface roughness.
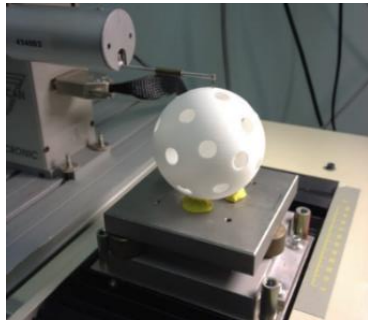

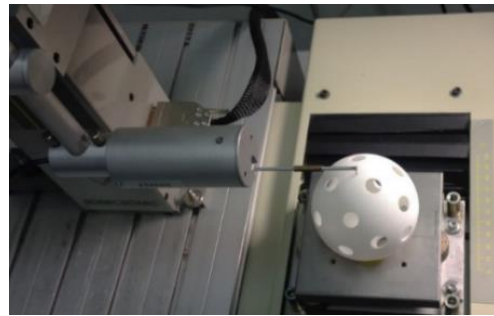Figure 41.Measurement of surface roughness with stylus device, front view

Figure 42. Measurement of surface roughness with stylus device, top view

6.3. Flight test

The flight of prototypes was studied by two different teams, performed by recording the shots in order to analyse the flight of the ball and compare it with commercial balls. The recorded shots provided the data for the analysis of trajectories and speeds, providing input for more specific calculations of aerodynamic coefficients.

6.3.1.Collaborating partners

The Sport and Technology group at Chalmers was contacted with the purpose of obtaining recommendations and contacts, providing the connection with Lindome IBK and Pixbo Wallenstam IBK. The shots performed in each team were recorded with GoPro Hero 3 in order to take videos with a high rate of frames per second, in this case 100 fps. The camera was also provided by Sports and Technology group.

6.3.2.Experimental Set up

The experimental set up for the recording was according to the Figure 43. The shooting point was positioned about 4-5m from a goal and the camera placed between the player and the goal having a wide angle configuration, see Figure 44.
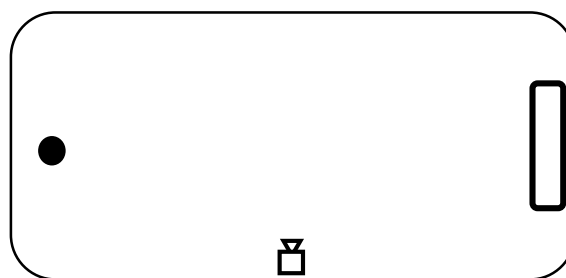
Figure 43. Experimental set up representation

The videos were loaded in the software Tracker and the shot frames were selected. The next steps were to select of a coordinate system and a fixed reference, as shown in Figure 44 plotted in pink colour. As a reference for the dimensions, a calibration line is settled. The diameter of the ball, 7,2 cm, was used as the calibration for both horizontal and vertical measurements, shown as blue lines in the Figure 44. Once the frames and coordinates system were settled, the software could recognize the ball object to track and evaluate different parameters such as position, speed and acceleration.

Figure 44. Video frame loaded on Tracker with Coordinate system and calibration bars.

6.3.1. Flight analysis

Using the open source software Tracker it was possible to obtain dynamic data from the videos and translate it into aerodynamic parameters for further analyse. The trajectory of the balls was easily followed by using a tool in the software that recognises the desired pixels, in this case the ball.

- **Experimental drag**

Based on the trajectory, the software calculated the vector of the speed in each point, defined by a magnitude and an angle respect to the horizontal axis. Also the acceleration was registered so the forces applied to the ball could be calculated by using Newton's second law, which states that the acceleration of an object is directly proportional to the net force applied on it and inversely proportional to the mass, Equation 6.

$$\vec{F} = m \cdot \vec{a} \tag{6}$$

By using the balance of forces on a solid body interacting with the aerodynamic forces, assumed to be drag and lift forces, also the corresponding coefficients were calculated. The diagram in Figure 45 represents the forces acting on the ball, where it is shown that from the decomposition of the forces, then it is possible to calculate both drag and lift.
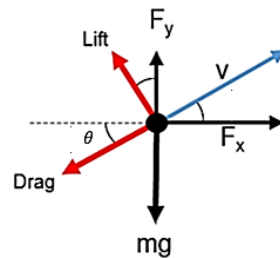

Figure 45. Force diagram applied to a body moving through a fluid

The resulting equations of balance in each direction are shown in Equation 7 and Equation 8. By solving the equation system, the drag and lift forces can be calculated as a function of the mass, acceleration and angle of the speed by means of the Equation 9 and 10.

$$\Sigma F_x = 0 \;\; ; \;\; F_x = D \cdot \cos\theta + L \cdot \sin\theta \tag{7}$$

$$\Sigma F_y = 0 \;\; ; \;\; F_y + L \cdot \cos\theta = D \cdot \sin\theta + m \cdot g \tag{8}$$

$$D = (a_y - g) \cdot m \cdot \sin\theta + m \cdot a_x \cdot \cos\theta \tag{9}$$

$$L = \frac{m \cdot a_x - D \cdot \cos\theta}{\sin\theta} \tag{10}$$

6.4. Results

6.4.1. Prototype 1

The first manufactured prototype had a good dimensional accuracy in general, as it can appreciated in Figure 46 which shows the detail of a hole. Regarding the surface, the layers were seen quite clearly in some parts of the ball. The most appreciable layers of powder are shown in Figure 47.

Figure 46. Detail of hole in the Prototype 1   Figure 47. Detail of layers visible on Prototype 1 surface

The main deficiency of this model was the weight, which was lower than expected according to tolerances for the IFF weight requirement. The sintered density was around 0,87 gr/cm^3, being lower than the values given by the equipment manufacturer.

It can be added here that the surface roughness was measured at an area where the layers are most visible and also at a section between holes that looks quite smooth. The results for both areas showed higher values than the certification requirement (around 25μm) and some polishing operations would be needed in order to be in accordance with the values for certification.

6.4.2. Prototype 2

The results for measurements on Prototype 2, performed as described in sections 6.2.1 and 6.2.2, showed that the requirements on weight and dimensions were fulfilled, as shown in Table 12.

Prototype 2					
Weight (g)	22.0562				
Measurements	**1**	**2**	**3**	**4**	**5**
Diameter (mm)	71.68	70.96	71.53	71.02	71.16
Holes (mm)	10.03	10.12	10.12	10.08	10.02

Table 12. Measured dimensions of the prototype 2.

This ball was then tested in Lindome Innebandy Club by the player Adam Widebert, Figure 48. The recording set up was as described in section 6.3.2, shown in Figure 48.

Figure 48. Adam Widebert performing the tests with the prototype

The commercial ball used as a reference was of type Aero+ from the manufacturer Salming (27), which had a structured surface with round dimples and internal reinforcements, Figure 49. Three shots were recorded with the prototype before the fracture shown in Figure 51 clearly proved that the material was not an appropriate choice regarding the durability of the product and that behaviour differs from the polyethylene materials considerably. Shots were also recorded with the commercial Aero ball at the same occasion and with the same recording set up.

| Figure 49. Aero+ ball | Figure 50. Chamfer ball | Figure 51. Prototype after the test |

The data extracted from the recorded videos with Tracker allows for comparison of the trajectories for the different shots. Even though the repeatability and the number of shots were not high enough to obtain reliable results, some similarities can be determined, see Figure 52.
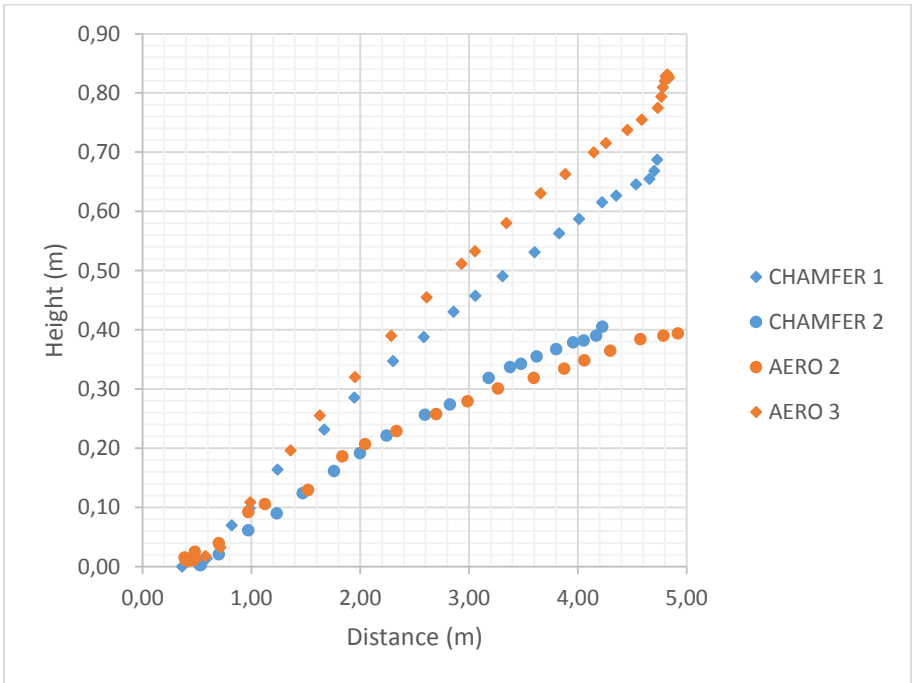

Figure 52. Trajectories comparing shot with Chamfer and Aero balls.

From the graphic it was clear that both balls behaved similarly and could be grouped in two pairs of shots: Chamfer 1- Aero 3 and Chamfer 2-Aero 3. The other two shots, Chamfer 3 and Aero 1 were discarded for further analysis, one due to the fracture of the ball and the other because there was no comparable shot with the Chamfer ball.

The trajectories corresponding to the shots Chamfer 1 and Aero 3 show a similar pattern for a part of the trajectory, see Figure 53. Consequently it was interesting to analyse the parameters that could cause the deviation. The speed profile showed a good fitting when compared in time evolution, Figure 54, therefore it could be possible that the shooting parameters for the launch were close.
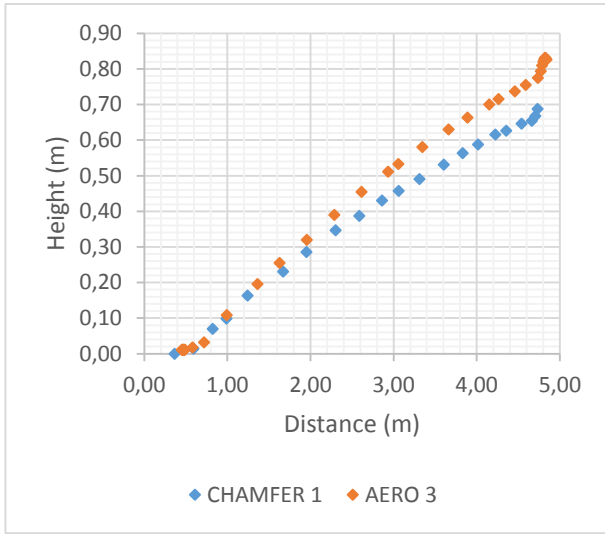

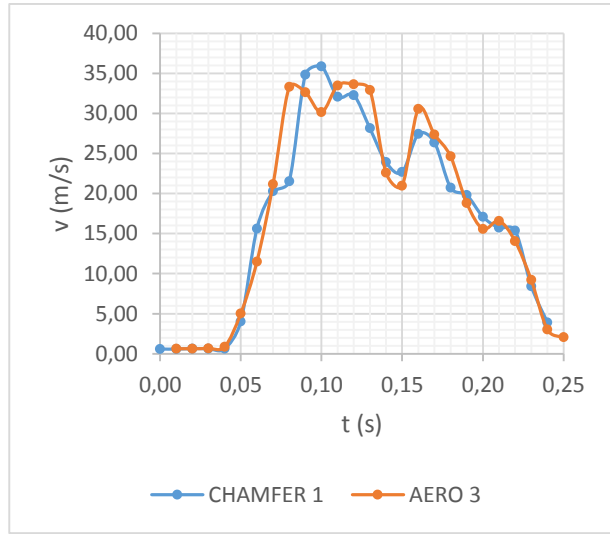Figure 53. Trajectories for Chamfer 1 and Aero 3

Figure 54. Speed as a function of time for Chamfer 1 and Aero 3

The drag coefficient was then analysed in terms of acceleration following the shot with the club where the ball reaches its maximum speed. The drag coefficient was calculated showing quite high values at low speed, decreasing rapidly with increasing speed and levelling out. The results were similar for both balls studied, see Figure 55.

The lift coefficient was calculated and plotted as a function of the speed, see Figure 56. It seems that for the Chamfer it had different lift coefficient values, see Figure 56, but this may be irrelevant considering the set up and the limited shots performed.
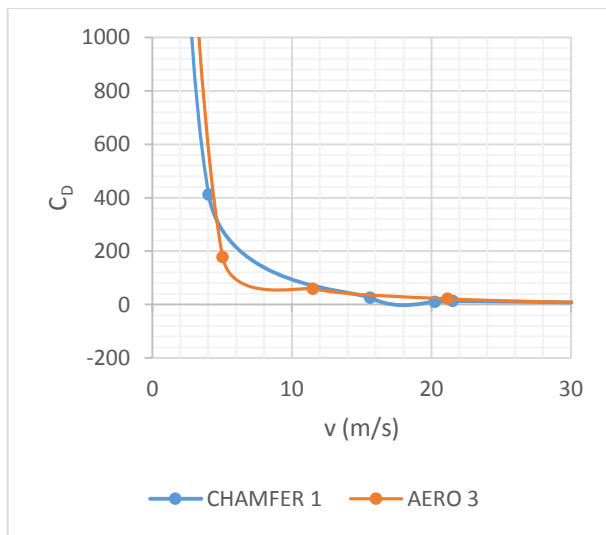

Figure 55. Drag coefficient as a function of speed,

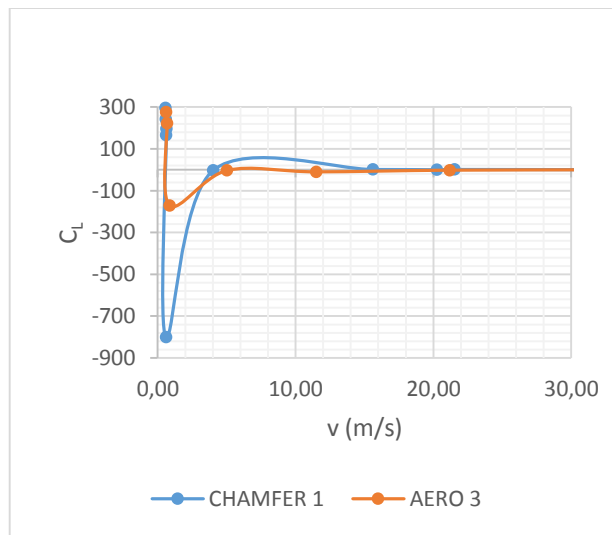corresponding to 0 to 0,1 seconds in Figure 54

Figure 56. Lift coefficient as a function of speed,

corresponding to 0 to 0,1 seconds in Figure 54

6.4.3. Prototype 3

The results for prototype 3 regarding the measurements described in sections 6.2.1 and 6.2.2 fulfil the requirements of weight and dimensions, shown on Table 13.

Prototype 3					
Weight (g)	22.3223				
Measurements	**1**	**2**	**3**	**4**	**5**
Diameter (mm)	71.61	71.30	71.51	71.69	71.57
Holes (mm)	10.13	10.11	10.19	9.88	10.06

Table 13. Measured dimensions of the prototype 3.

The prototype 3 was used for shots at Pixbo Wallenstam IBK by the player Sara Helin. The recording was as described in section 6.3.2, shown on Figure 57. Here, five shots were recorded with the prototype and three shots with a commercial ball.

Figure 57. Sara Helin performing the test, position points generated by the software Tracker

The ball used as a reference was of type Crater, from the manufacturer Renew Group (28). The ball had a structured surface with linear grooves in a parallel and meridian distribution. After the 5th shot, the prototype 3 showed a crack between holes, see Figure 60.

Figure 58. Crater ball

Figure 59. Chamfer ball

Figure 60. Prototype after the test

The data obtained from the recorded shots was analysed with the software Tracker, by selecting the ball as moving object each position has been determined, as shown on Figure 57 by the points and numbers in red. The values of position, speed and acceleration were shown by Tracker, in graphic and numerical. The Figure 61 shows all the shots performed in the same coordinate system.

A first observation was that the shots had a good repeatability and the trajectories of the prototype were similar to some shots performed with the reference ball type crater. From the Figure 61 it was possible to establish similarities for four trajectories connecting the prototype ball and the commercial ball. The pairs Chamfer 2- Crater 1 and Chamfer 3- Crater 2 were further analysed in order to determine the aerodynamic characteristics.
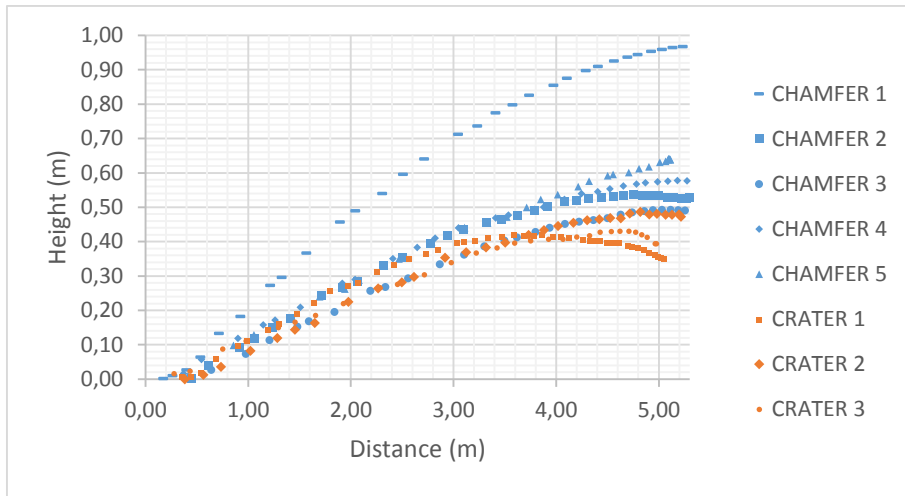

Figure 61. Trajectories comparing all shots with Chamfer and Crater balls.

The trajectories corresponding to the shots Chamfer 2 and Crater 1 were observed to have similar pattern for half of the trajectory, Figure 62. The corresponding speed profiles were calculated to be different, the chamfer geometry being higher for a large part of the time studied, see Figure 63. The Drag coefficient calculated was, however quite similar in comparison, see Figure 64.
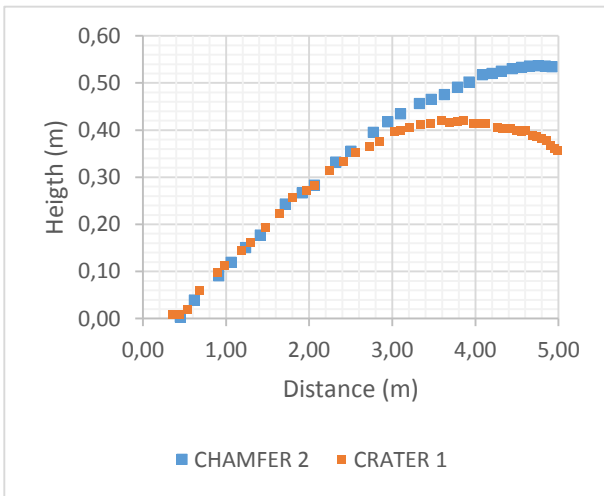

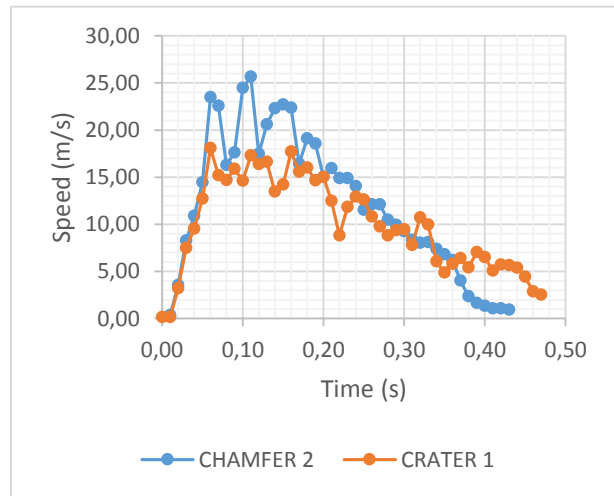Figure 62. Trajectories for Chamfer 2 and Crater 1

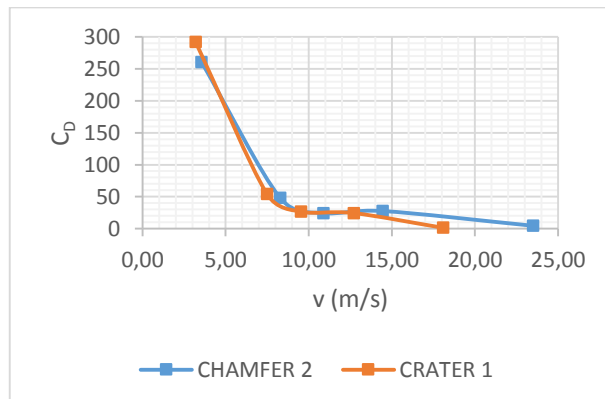Figure 63. Speed as a function of time for Chamfer 2 and Crater 1

Figure 64. Drag coefficient as a function of speed in the acceleration of the ball after hit

33

The major differences between the speeds from trajectories shown in Figure 62 were observed between 3 and 4 m distance from the shooting point. This interval is highlighted in Figure 65, showing a deviation in the trajectory about 10 cm and a general difference in speed of about 5 m/s, Figure 66.
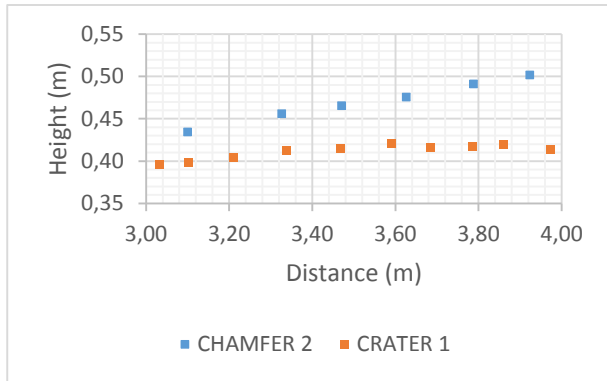

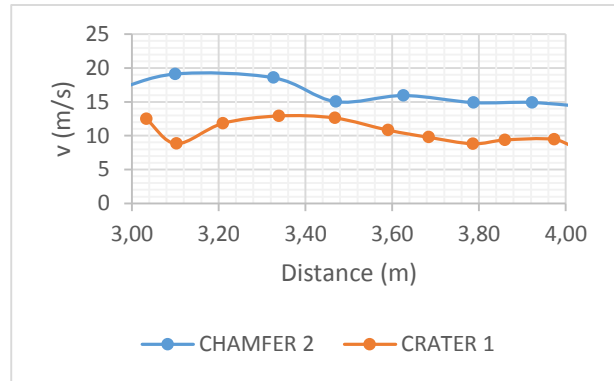Figure 65. Trajectory deviation, from 3 to 4 m from shooting point

Figure 66. Speed deviation, from 3 to 4 m from shooting point

Correlating these points with their corresponding drag and lift coefficients, the deviation of the trajectory can be explained by a peak in the drag for the Crater ball, Figure 67. The peaks likely correspond to a sudden reduction of the speed, influenced by the rise in the drag force. Also, the calculated lift values were different, see Figure 68.
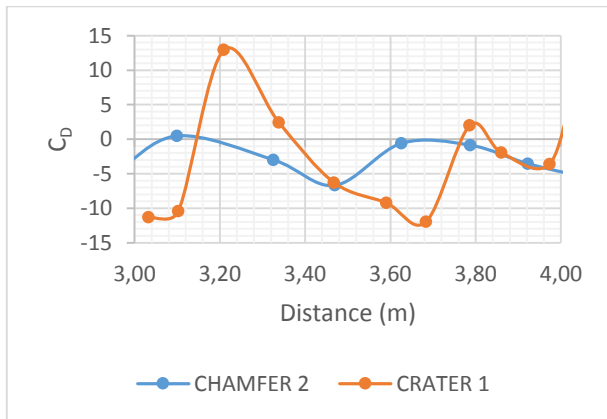

Figure 67. Drag as a function of the position ,from 3 to 4 m from shooting point
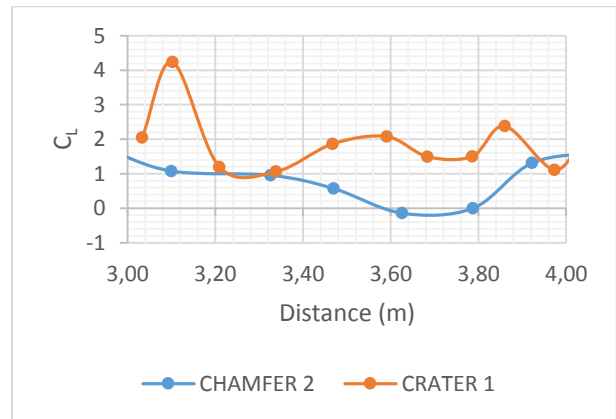
Figure 68. Lift as a function of the position, from 3 to 4 m from shooting point

Considering this behaviour of the chamfer ball, it can be argued that the lower Lift coefficient and lower Drag coefficient maintain the trajectory at higher speed. Even if the lift values for the Crater ball are higher (the orange dots in Figure 70), the trajectory describes a lower curve. Moreover, the drag coefficient shows a noticeable variation when analysed in a speed context in the aforementioned points, Figure 69. This variation of drag values for the same speed can be explained by a different rotational rate likely influencing the drag.

Figure 69. Drag coefficient for different speed points

Figure 70. Lift coefficient for different speed points

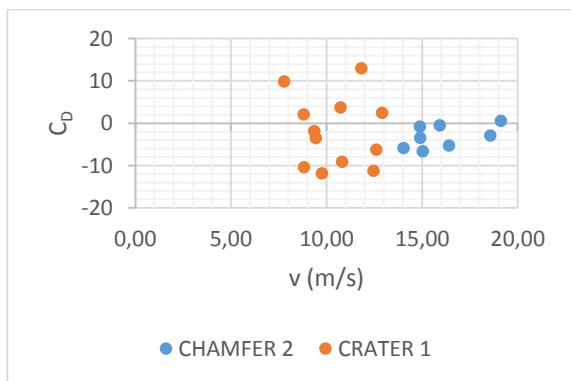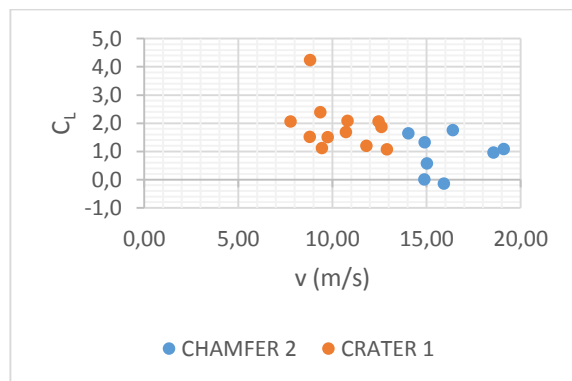The trajectories corresponding to the shots Chamfer 3 and Crater 2, Figure 71, show a very similar pattern. Consequently, the study of the speed and aerodynamic parameters may imply that the prototype ball had a precision behaviour. The speed profile showed a good fitting as well, Figure 72, so it could be possible that the shooting parameters for the launch were close and the results obtained could be considered to be reliable for the aerodynamic studies.
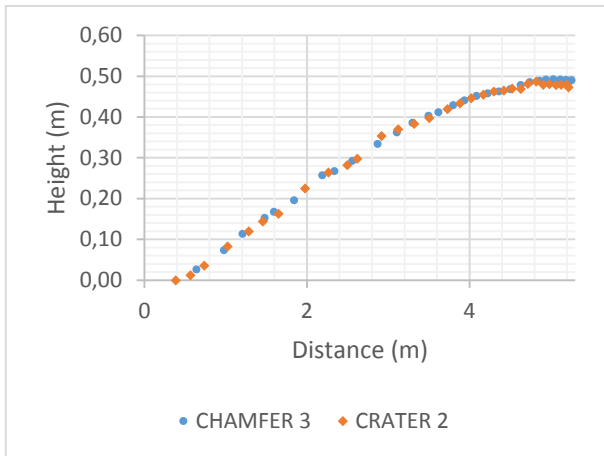
Figure 71. Trajectories of Chamfer 3 and Crater 2
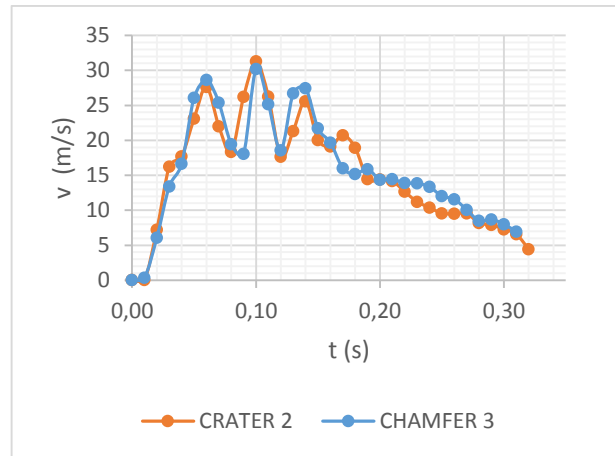
Figure 72. Speed as a function of time for Chamfer 3 and Crater 2

The acceleration of the balls at the shot is really close and in general the speed profile has a common appearance, with smaller deviations during deceleration. Similar values for the drag and lift coefficients were seen for both balls. The drag coefficient plotted as a function of the speed, Figure 73, was quite similar. The minor differences in speed profile appeared in the interval between 0,2 s and 0,25 s, see Figure 72, may be due to errors in measurements. A closer study of this interval, Figure 74 and Figure 75, reveals no consistent differences.

Figure 73. Drag coefficient as a function of speed for acceleration stage

Figure 74. Drag coefficient for different speed points between 0,20 and 0,30 s.

Figure 75. Lift coefficient for different speed points between 0,20 and 0,30 s.

35

7. Analysis of the Results

The aim of this thesis work was to suggest an appropriate product development for Floorball Equipment, specifically improving the balls for indoor and outdoor play. The method followed during the work was mostly based on computer design and compute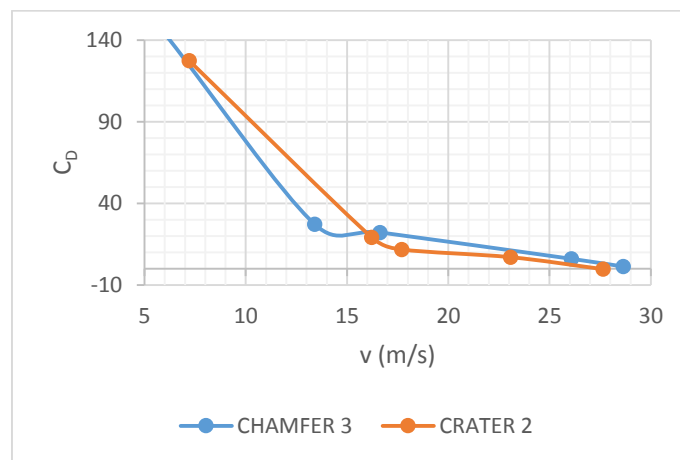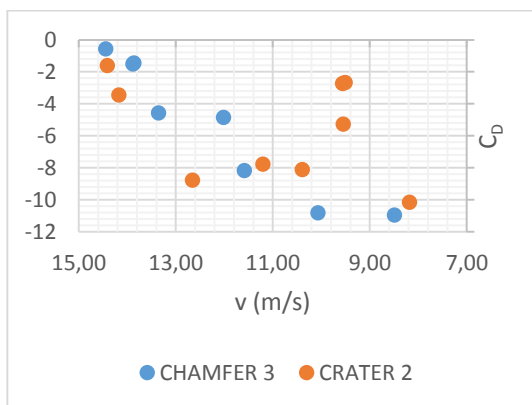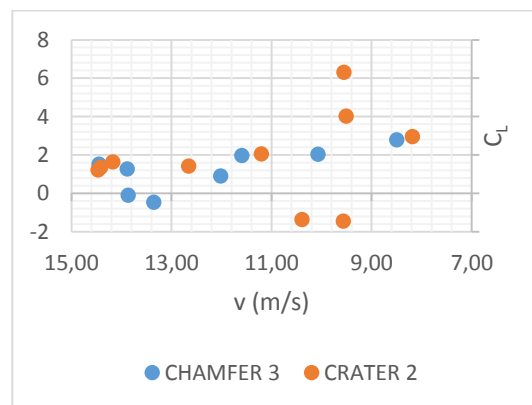r fluid dynamics simulations for the evaluation of geometries prior to test the selected alternative after manufacturing prototypes.

The major finding in this work was that the modified geometry of the holes in a Floorball ball can improve the design and may lead to a more predictable shot. The flight of the ball through the air is influenced by the aerodynamic forces, known as drag and lift, therefore the study of them has been an important issue for many authors in the field from the early research of Achebach, (29) and (30), to the more specific in sports balls by Metha (22) and consequently a determinant part of this research.

The review of previous development shows that the tendency has been to reduce the drag by creating dimpled surfaces, however the present research implies that such reduction is possible as well by modifying the geometry of the holes.

The Evaluation of the Design, section 4, shows that the reduction of the diameter of the holes may likely lead to a faster and more stable flight for the ball influenced by a reduced drag force. It was stated as well that different features of the holes can reduce the drag without compromising the possible certification as they maintain the required dimensions. The selected geometry for prototype was the design with a chamfer feature inside the holes as it was one of the best solutions from the simulation results.

The analysis of the flight performed with the prototypes showed that it behaved similarly to commercial precision balls, Figure 76, also having a good repeatability even if the number of tests was limited.
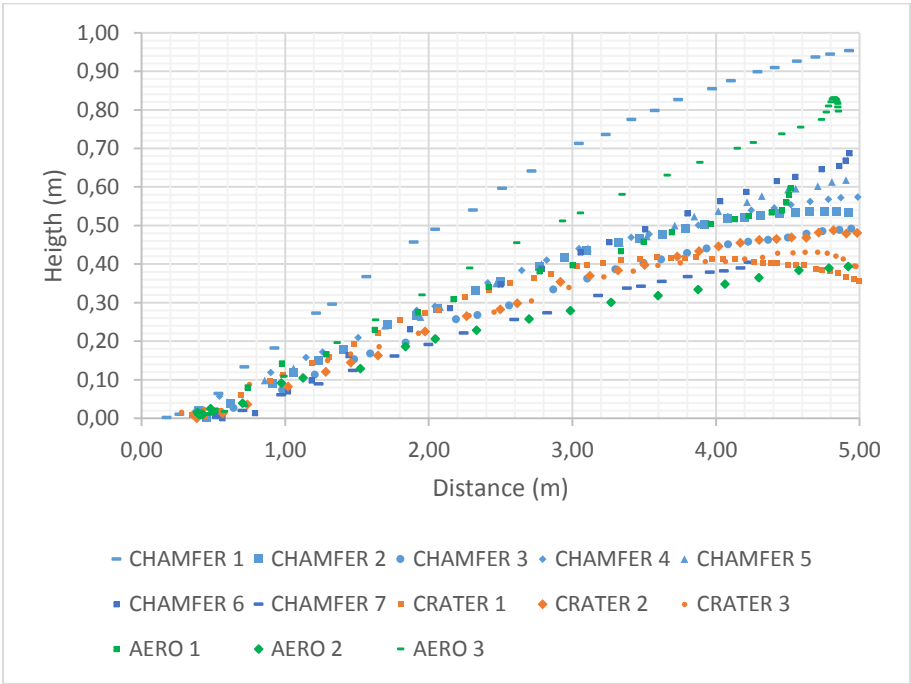
Figure 76. Trajectories comparing Chamfer ball with precision balls.

In an effort to better evaluate the performance of the prototype, compared with the other precision balls, parameters such as speed and aerodynamic coefficients have been analysed in detail in the corresponding sections, 6.4.2 and 6.4.3.

The results of this evaluation provide support for the precision behaviour of the chamfer ball and correlate with the theoretical explanations and research carried out by Metha (22), explaining that the drag coefficient should be reduced for a better performance in sports balls.

8. Discussion

The choice of prototyping the design with the chamfer inside the holes was supported by favourable simulations of the drag reduction. Even if the simulations were compared with the basic geometry according to SPCR 11, Figure 77, it was worth it to try to verify the design in real environment. If this design could perform as shown in the simulations it would have been possible to certify the potential product fulfilling the current dimension requirements.

Figure 77. Drag coefficient as a function of speed in m/s.

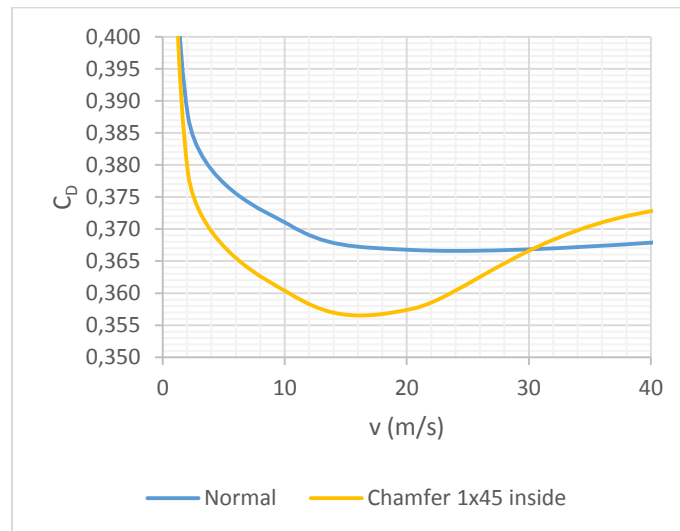The manufacturing of the prototype with the Selective Laser Sintering process seems to achieve good accuracy for the dimensions. The high roughness values obtained on the surface could have been beneficial for the performance of the ball during the flight. Achenbach (29) studied the influence of the roughness parameter on spherical surfaces as a determinant factor for the Critical Reynolds number and consequently obtaining a great drag reduction, or Drag crisis, at lower speeds.

The material selected for the manufacturing of the prototype was shown to be far too brittle for play. It may be noted that the equipment manufacturers contacted stated that the Selective Laser Sintering with Polyamide 2200 should provide a good impact resistance.

The ideal prototype for the flight test would likely be made of polyethylene, in order to have better durability. New prototypes of polyethylene may possibly also be evaluated in terms of rebound and breaking stress. Further, the manufacturing of a ball in polyethylene from a prototype point of view would be expensive if the traditional injection moulding would be used, therefore the Freeformer process type according to company Arburg (19) would be an interesting manufacturing process to try as it is stated to combine a low time and cost for a prototype series but with the advantage of using standard material granulates.

9. Conclusions

- Geometries of new designs for Floorball balls have been evaluated by using CFD simulation, leading to interesting results for an improved predictability of the ball during flight.

- In contrast to previous research and design, the present work implies that it is possible to obtain a drag reduction by modifying the geometry of the holes. For significantly reduced drag during flight, smaller holes and inside chamfer edges are suggested.

- A prototype ball designed for the purpose of this thesis work and manufactured with AM technologies has been tested and compared with current precision balls, confirming an improved performance.

10. Further Work

During the development of the CFD simulations, the adjusted geometries have been compared with the current basic model of ball and this may cause limitations in the reductions achieved. Consequently, a suggestion for further development is to compare the new designs with precision balls in both simulation and real environments for verification of a higher reduction of the drag and thus a better precision ball.

The experimental measurements during the flight test are influenced by the available frame rate of the camera used in the experiments. The frame rate used (100 frames per second) seems to not be enough for a good determination of the position of the ball. In some frames, the ball was blurred and the software could not properly recognise the ball and consequently the related parameters may have some error. The rotation of the ball was not measured, therefore the values of drag and lift coefficient could not be identified in this context and compared with the simulation results.

The use of a high speed camera or at least a frame rate over 100 frames per second would be a suggestion for future research in order to obtain more accurate results for the measurements and dependent calculations. Moreover, the performance of a greater number of shots would give more consistent results.

The prototypes produced by SLS had low durability. A suggestion for the future would be to manufacture prototypes in polyethylene with the Freeformer process, for further evaluation of suggested new ball geometries during play.

11. References

1. **SP Technical Research Institute of Sweden.** Testing and Certification of Floorball Equipment . *Floorball Equipment Web Site.* [Online] 13 April 2015. http://floorball.sp.se.

2. **International Floorball Federation.** Member Statistics. *International Floorball Federation.* [Online] 10 April 2015. http://www.floorball.org/pages/EN/Member-Statistics.

3. **Chalmers University of Technology.** Innebandy. *Chalmers Sport & Teknologi.* [Online] 16 April 2015. http://www.sportteknologi.se/innebandy.

4. **Karlsson, Jonny.** *Analysis of Floorball sticks using high speed camera and Abaqus.* Göteborg : Chalmers University of Technology, 2011.

5. **Lindstöm, Mats.** *Improved material performance in floorball sticks.* Göteborg : Chalmers University of Technology, 2015.

6. **Salming Sports AB.** *Salming Floorball.* [Online] 8 April 2015. http://www.salmingfloorball.com.

7. **International Floorball Federation.** News: UNIHOC continues as IFF Sponsor – 18.12.2014. *International Floorball Federation.* [Online] 16 April 2015. http://www.floorball.org/news.asp?id_tiedote=4223.

8. **RENEW GROUP SWEDEN AB.** News. *Unihoc.* [Online] 8 April 2015. http://www.unihoc.se/news.html.

9. **Bergström, Joacim.** *WO/2012/126442* Sweden, 2012.

10. **International Flooball Federation and SP Technical Research Institute of Sweden.** *Material Regulations Certification Rules for IFF-marking of Floorball Equipment SPCR 011.* s.l. : International Floorball Federation, 2014.

11. **Kalpakjian, S. & Schmid, S.R.** 19.3 Injection Molding. *Manufacturing engineering and technology.* Singapore : Prentice Hall, 2010.

12. **Troughton, Michael John.** *Handbook of Plastics Joining: A Practical Guide, Second Edition.* s.l. : William Andrew, 2008.

13. *Additive Manufacturing Advances.* **Wohlers, Terry.** 2012, Manufacturing Engineering, 148(4), pp. 55-56,58,60-63.

14. *3D printing builds up its manufacturing resume.* **Caffrey, T., & Wohlers, T.** 2014, Manufacturing Engineering, 152(6), pp. 61-62,64-68.

15. *Why 3D-Printing is a Real Game Changer in Modern Medicine.* **Semetaite, Juste.** Highlands Ranch : Advantage Business Media, 2014, Product Design & Development.

16. **Elmia.** Elmia Polymer. *Elmia Polymer.* [Online] [Cited: 24 April 2015.] http://www.elmia.se/en/polymer/.

17. **Addema AB.** About Addema. *Addema Web site.* [Online] [Cited: 23 April 2015.] http://addema.com/about-addema.

18. **Prototal AB.** Methods Plastic. *Prototal Web site.* [Online] [Cited: 23 April 2015.] http://www.prototal.se/en/home/.

19. **Arburg GmbH .** Additive manufacturing. *Arburg Web site.* [Online] [Cited: 24 April 2015.] https://www.arburg.com/products-and-services/additive-manufacturing/.

20. **Floorball4all.** Floorball4all. [Online] 13 April 2015. http://www.floorball4all.info.

21. **Kaufman, Hansjörg.** *Interview: Hansjörg Kaufman, Floorball4All.* [interv.] Speedhoc. 29 May 2013.

22. **Metha, Rabindra D.** Sports ball aerodynamics. *Sport aerodynamics.* Wien : Springer, 2008.

23. *A review of recent research into aerodynamics of sport projectiles.* **Goff, John Eric.** 16, 2013, Sports Engineering, pp. 137-154.

24. *Ludwig Prandtl's Boundary Layer .* **Anderson, John D. Jr.** 12, 2005, Physics Today , Vol. 58, pp. 42-48.

25. **Mateos Fernández, Sara.** *Innebandyboll. 2015/0364* Sweden, 02 10 2015. Innebandy Ball.

26. **International Flooball Federation and SP Technical Research Institute of Sweden.** Appendix 1 Section 5.3. *Material Regulations Certification Rules for IFF-marking of Floorball Equipment SPCR 011.* s.l. : International Floorball Federation, 2014.

27. **Salming Floorball.** Aero Balls. [Online] [Cited: 17 September 2015.] http://www.salming.com/en/floorball/accessories/balls/.

28. **Renew Group Sweden AB.** Renew Group Sweden AB. [Online] [Cited: 17 September 2015.] http://renewgroup.se/.

29. *The effects of surface roughness and tunnel blockage on the flow past spheres.* **Achenbach, Elmar.** 1974, Journal of Fluid Mechanics, Vol. 65, pp. 113-125 .

30. *Experiments on the flow past spheres at very high Reynolds numbers.* **Achenbach, Elmar.** s.l. : Cambridge University Press, 1972, Journal of Fluid Mechanics, Vol. 54, pp. 565-575.